Fabrication of graphene oxide scrolls and other architectures

Wu, Jumiati

2014

Wu, J. (2014). Fabrication of graphene oxide scrolls and other architectures. Doctoral thesis, Nanyang Technological University, Singapore.

https://hdl.handle.net/10356/62940

https://doi.org/10.32657/10356/62940

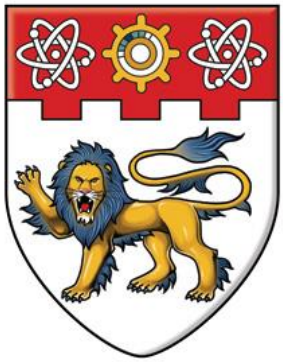

NANYANG TECHNOLOGICAL UNIVERSITY

FABRICATION OF GRAPHENE OXIDE SCROLLS AND OTHER ARCHITECTURES

JUMIATI WU

SCHOOL OF MATERIALS SCIENCE AND ENGINEERING

2014

FABRICATION OF GRAPHENE OXIDE SCROLLS AND OTHER ARCHITECTURES

JUMIATI WU

2014

FABRICATION OF GRAPHENE OXIDE SCROLLS AND OTHER ARCHITECTURES

JUMIATI WU

JUMIATI WU

SCHOOL OF MATERIALS SCIENCE AND ENGINEERING

A thesis submitted to the Nanyang Technological University in partial fulfillment of the requirement for the degree of

Doctor of Philosophy

2014

ACKNOWLEDGEMENT

My utmost gratitude goes to my supervisor, Professor Zhang Hua, for his continuous support and his constructive advice as well as guidance during my PhD candidature period. His committed supervision has led me to accomplish what I have today. I also extend my gratitude to Professor Subbu S.Venkatraman for his support towards my PhD. I also would like express my gratitude to Dr. Li Hai for his mentorship during my PhD candidature. His constant support and guidance throughout has inspired and enlightened me on the excellency of research.

I also thank my former and current fellow group members Dr. Qi Xiaoying, Dr. Huang Xiao, Mr. Fan Zhanxi, Mr. Yang Jian, Dr. Cao Xiehong, Ms. Huang Ying, Dr. Wu Xuejun, Dr. Liu Juqing, Mr. Ma Qinglang, Mr. Zhang Xiao, Mr. Chen Bo, Mr. Tan Chaoliang, Mr. Chen Junze, Mr. Zeng Zhiyuan, Mr. He Qiyuan, Dr. Yin Zongyou, Mr. Cipto Liusman, Dr. Lu Gang; for their kind help and supportive discussion. In addition, I would like to show my appreciation towards all the technicians in the School of Materials Science and Engineering especially Organic Materials Lab of Nanyang Technological University, for their kind and continuous support.

Last but not least, I am especially grateful to my fiancée, Mr. Thi Ha Kyaw, for his continuous support and positive input. My deepest thanks go to my family for their unconditional understanding and support. This thesis is dedicated to them, for their unwavering love and faith.

TABLE OF CONTENTS

LIST OF ABBREVIATIONS AND SYMBOLS

Graphene Oxide	GO
Reduced Graphene Oxide	rGO
Carbon Nanotube	CNT
Single Walled Carbon Nanotube	SWCNT
Carbon Nanoscroll	CNS
Polydimethylsiloxane	PDMS
Poly (L-Lactic Acid)	PLLA
Self-Assembled Monolayers	SAMs
16-Mercaptohexadecanoic Acid	MHA
Octadecanethiol	ODT
Dichloromethane	DCM
Octadecyltrimethoxysilane	OTS
1-Octadecanethiol	ODT
11-Mercapto-1-Undecanol	MUO
4-Aminothiophenol	ATP
Copper	Cu
Atomic Force Microscopy	AFM
Transmission Electron Microscopy	TEM
Scanning Electron Microscopy	SEM
Microcontact Printing	μCP
Current	I
Voltage	V

LIST OF FIGURES

LIST OF TABLE(S)

ABSTRACT

Graphene, a two-dimensional material made of entirely carbon atom in sp^2 hybridization has been introduced in 2004. Due to its unique and excellent electrical, mechanical and optical properties, graphene is popularly researched as materials of interest to be used in variety of applications. As a two-dimensional material, graphene is considered as building block for other carbon based materials. Graphene can wrap around itself and form buckyballs, roll to form carbon nanotube (CNT), and stack to form graphite. All these different architectures of carbon materials result in distinctive properties. Hence, it is exciting to fabricate new architectures based on carbon materials.

Novel graphene architecture such as carbon nanoscroll or graphene scroll is recently reported. This architecture is similar to CNT. Both of them are made of rolled graphene. However, CNT displays a closed cap configuration while carbon nanoscroll or graphene scroll shows an open cap configuration. Molecular combing is applied on two-dimensional material of GO sheets for the first time. Molecular combing of GO sheets in aqueous solution is executed on various hydrophobic substrates which consequently results in formation of GO scrolls. The obtained GO scroll is then characterized by using optical microscopy, Raman spectroscopy, atomic force microscopy (AFM) and transmission electron microscopy (TEM). Molecular combing technique has produced aligned individual GO scrolls with high density easily. The successful fabrication of GO scroll is found to be controlled by the substrate's hydrophobicity as well as water which was the solvent of GO sheet solution. A device based on a single reduced GO scroll is produced with gold as

electrodes and further utilized as NO_2 gas sensor. As an active material, rGO scroll has demonstrated the ability to detect NO_2 as low as 0.4 ppm with detection limit of 56 ppb.

Micro-contact printing of hydrophilic 16-mercaptohexadecanoic acid (MHA) on Au substrate followed by passivation of hydrophobic 1-octadecanethiol (ODT) revealed the hydrophilic-hydrophobic region. By performing molecular combing of GO sheets on hydrophilic-hydrophobic patterned substrates, novel GO architecture is observed. Molecular combing on MHA dot-patterned substrate results in the beaded GO string, which is characterized by optical microscopy, scanning electron microscopy (SEM), AFM, Raman spectroscopy and TEM. The resulting GO architecture can be easily tuned by controlling the size and shape of hydrophilic region. Moreover, GO sheets has also been demonstrated to favor hydrophilic area and thus selectively reside and adopt hydrophilic area size and shape, such as line and cross pattern. The concentration of GO sheets and molecular combing speed are two factors to tune the density of resulting beaded GO strings. In addition, the size of GO sheets is also crucial to the formation of beaded GO string. The single beaded rGO string based device is also fabricated, which gives better NO_2 gas detection limit (5.8 ppb).

In addition, the GO scroll mesh is produced by stacking high density GO scrolls which are aligned in vertical and horizontal directions. Vertically aligned GO scrolls are stacked on horizontally aligned GO scrolls by using two-dimensional material transfer method. The resulting GO scroll mesh is shown to be made of well-connected GO scrolls in large area as characterized by optical microscopy, Raman spectroscopy and AFM. The GO/rGO scroll mesh is structurally stable and therefore transferrable onto flexible substrates such as PET. Optical transparency and sheet resistance of GO/rGO scroll mesh

are excellent due to its mesh/network structure and the conductivity of rGO. The rGO scroll mesh based device is fabricated, which shows remarkable electrical stability with multiple bending tests.

Chapter 1:

Introduction

1.1 Background and Motivation

Since the first observation of graphene in 2004 by Novoselov *et. al.*,[1] graphene has been actively researched. Single and few layer graphene were successfully fabricated by mechanical exfoliation of graphite. Graphene is made of sp^2 hybridized carbon atoms arranged in honeycomb lattice. Graphene's electrical property is found to be unique, which is semi metal with overlap in its conductance and valence band. Graphene carrier mobility at room temperature is found to be between 3,000-10,000 $cm^2/V{\cdot}s$ with carrier density of up to 3×10^{13} cm^{-2}.[1] Another study yielded graphene's thermal conductivity of around 5,300 $W/m{\cdot}K$.[2] Graphene mechanical properties is also measured with AFM and resulted with Young's modulus of E = 1.0 TPa and breaking strength of 42 $N{\cdot}m^{-1}$.[3] Graphene has also shown an excellent optical transmittance with opacity of 2.3% and which increased by 2.3% for each additional layer number.[4] Graphene with its outstanding properties are therefore considered as potential material in many applications such as supercapacitor,[5-7] lithium battery/storage,[8-10] hydrogen storage,[11-12] chemical/gas sensor,[13-19] etc.

As graphene possess excellent properties, its synthesis method has been widely explored. A synthesis method to produce graphene in high quality and high yield is highly sought. Chemical vapor deposition (CVD) technique has been able to produce high quality graphene over a large area[20] however the as-prepared graphene need to be transferred onto appropriate substrates for application purposes. Solution based graphene is therefore

preferred for ease of processing. Graphene oxide (GO) which is produced by modified Hummers' method[21-23] has been reported to produce large sheets of GO in high yield. This synthesis method is popular amongst researcher as it is solution processable, high yield, and its' ability to be reduced and results in reduced graphene oxide (rGO) which is conductive.

Graphene in planar sheet form; it is thought as building material for carbon materials in other dimensionalities.[24] Two-dimensional (2D) graphene sheet can be made into zero-dimensional (0D) buckyballs by wrapping, one-dimensional (1D) carbon nanotube (CNT) by rolling and three-dimensional (3D) graphite by stacking as depicted in Figure 1 - 1. In its other dimensionality such as 0D, 1D and 3D, each exhibits unique properties on its own. In 0D form, the most commonly found buckyballs which is buckminsterfullerene (C_{60}) is a semiconductor with band gap ranging from 1.5 - 2.3 eV.[25-26] In the other hand, armchair single-walled carbon nanotube (SWCNT) is found to be metallic, [27-28] 3D graphite is semi metal (~40 meV gap overlap)[29] while 2D graphene is a semiconductor with zero band gap (~4 meV gap overlap).[1]

A recently introduced graphene architecture resulting from scrolling of graphene/GO sheets is referred to as carbon nanoscroll (CNS) or graphene scroll. This architecture can be differentiated from CNT by its open cap configuration. The distinctive structure of graphene scroll may results in unique properties on its own. Easy and simple fabrication of graphene scroll is introduced in this thesis and its potential as gas sensing material is demonstrated. Further variation in graphene scroll architecture, such as beaded GO string is fabricated and its performance as gas sensor device is compared to graphene scroll. Graphene scroll mesh is also produced and its potential application as transparent and flexible electrode is demonstrated.

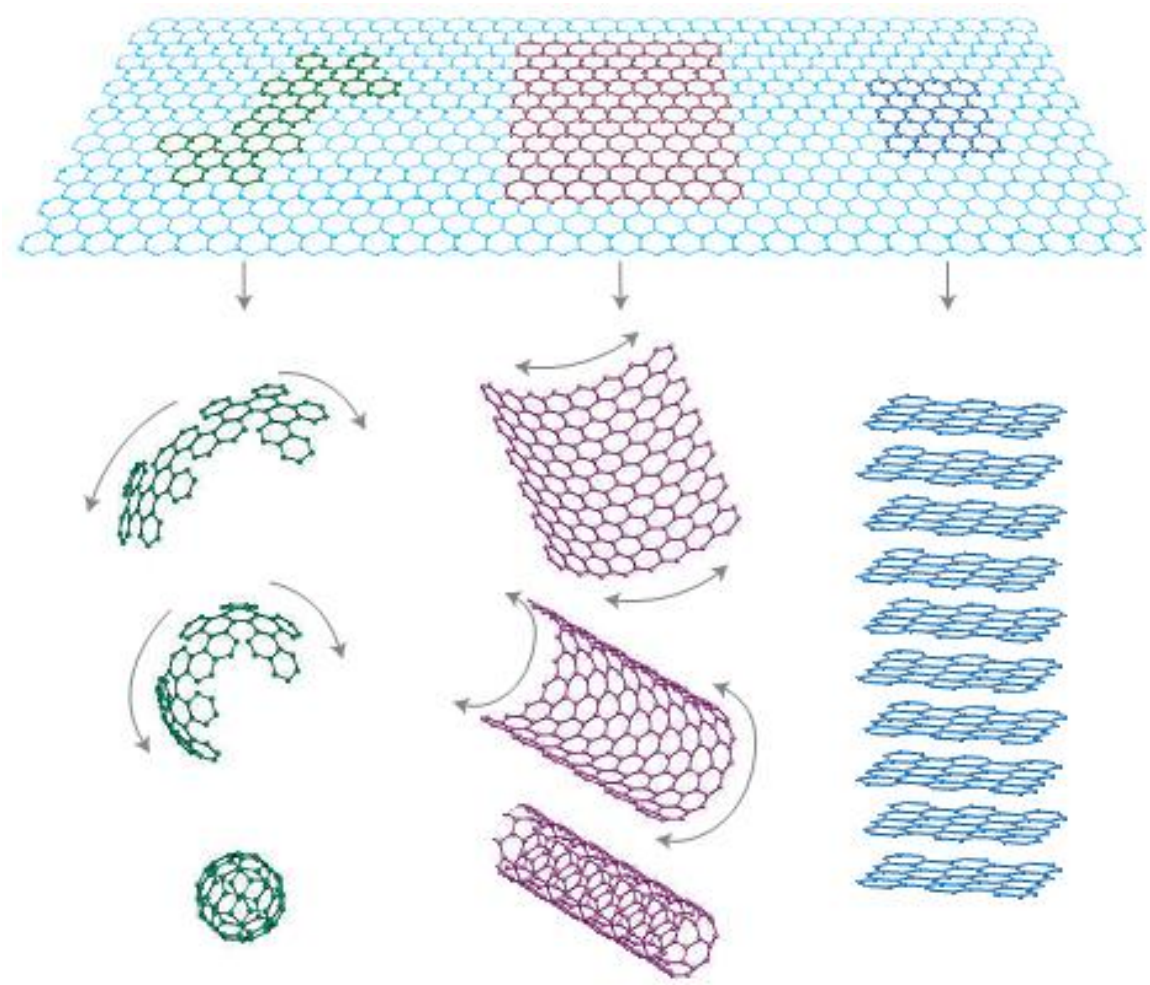

Figure 1 - 1. Two-dimensional (2D) graphene as building material for other carbon based architecture such as 0D fullerenes (C_{60}), 1D carbon nanotube (CNT), and 3D graphite. Reprinted with permission from Nature Publishing Group.[24]

1.2 Research Objective and Scope

New graphene architectures may contribute to unique and interesting properties of carbon based materials and its current limitations in fabrication techniques of CNS/graphene scroll has inspired the research works done in this thesis. Main objective of this research work is to achieve a high quality and high yield fabrication of new graphene

architectures including graphene scrolls. In order to achieve the objective, three approaches have been proposed below.

First approach is to fabricate graphene oxide (GO) scroll by using molecular combing technique on hydrophobic substrate. It aims to produce high quality and well-aligned GO scroll in high yield. Molecular combing is reported previously as a technique to stretch and align DNA strands on hydrophobic substrates. The receding water is proposed to stretch coiled DNA strands. Thus, the movement of water meniscus during molecular combing might supply energy for scrolling action. Therefore, applying this technique onto 2D GO sheets is predicted to result in the formation of well aligned GO scrolls with certain density which is possible to be controlled by the concentration of GO sheets in solution.

Second approach is to introduce hydrophilic-hydrophobic patterned region as a substrate during molecular combing of GO sheets. It aims to produce novel GO architecture and to control placement of GO sheets on hydrophilic-hydrophobic patterned area simultaneously. Molecular combing of GO sheets on hydrophilic-hydrophobic patterned substrate instead of hydrophobic substrate is expected to result in novel GO architecture due to different interaction between GO sheets and hydrophilic or hydrophobic area of substrate. At the same time, controllable placement of GO sheets can be investigated.

Third approach is to fabricate high density GO scrolls combed on horizontal and vertical directions. It aims to fabricate GO scroll mesh architecture made of high density GO scrolls. GO scrolls can be produced in high density and well-aligned in certain direction easily with molecular combing. Therefore, GO scroll mesh is anticipated to be fabricated by performing molecular combing of highly concentrated GO sheets in aqueous solution to produce high density GO scrolls in both vertical and horizontal direction.

All the prepared graphene architectures are characterized by optical microscopy (OM), Raman spectroscopy, atomic force microscopy (AFM), scanning electron microscopy (SEM) and transmission electron microscopy (TEM) to study its morphology and its structure.

1.3 Organization of the Thesis

Chapter 1 introduces the importance of graphene with its excellent properties as potential material for various applications. The objective and scope of the research work presented is discussed with fabrication of novel graphene architectures as main goal.

Chapter 2 reviews the relevant reports on research works performed previously. It starts with short introduction of graphene and its synthesis method to produce graphene oxide. Previous reports on fabrication method of CNS or graphene scroll are discussed. Molecular combing, micro-contact printing and various transfer techniques are also introduced.

Chapter 3 presents the materials, methodology, instrumentation as well as experimental procedures performed in this thesis. Characterization methods of the resulting GO architectures are also described.

Chapter 4 explains the fabrication and characterizations of GO scrolls as well as novel graphene architectures such as beaded GO string. Application of these architectures in gas sensing is demonstrated. Fabrication and characterization of GO scroll mesh is also presented along with its potential application as transparent and flexible electrode.

Chapter 5 presents the summary and conclusion of the research works described in previous chapters. In addition, the recommendations for future works are also introduced.

1.4 Main Contributions of the Thesis

Main contributions of the research works presented in this thesis are described below:

1. A first demonstration of molecular combing on 2D material (graphene oxide)
2. Fabrication of well aligned graphene oxide scroll in high yield by using simple technique
3. First report of beaded GO string and graphene scroll mesh

Chapter 2:

Literature Review

2.1 Introduction to Graphene and its Synthesis Methods

Graphene is widely known as 2D material made of carbon atom packed in honeycomb lattice with one atom thickness. As it holds excellent mechanical, optical and electrical properties, high quality/defect free graphene is highly sought. Various synthesis methods to produce graphene have been reported. Single layer graphene can be produced by mechanical exfoliation of highly oriented pyrolytic graphite (HOPG).[1] The as-produced graphene resulted in high quality graphene with minimum defects and therefore it is used in numerous intrinsic properties investigations.[1-4] In the other hand, the as-produced graphene has very low yield. Therefore, even though mechanically exfoliated graphene is of high quality but its' low yield hinders the possibility of these graphene to be used as viable material for various applications. High quality graphene synthesis has also been achieved by annealing of SiC wafer at high temperature (> 1000 ^{o}C).[30-31] However, this synthesis technique has high cost due to the substrate and temperature used.

Liquid[32-34] and thermal[35] or electrochemical[36] exfoliation of graphene has been reported to produce graphene in large quantity. However, these wet exfoliation techniques results in residual surfactant which are difficult to remove and therefore impact the properties of the resulting graphene negatively. Chemical vapor deposition (CVD) technique is also been shown to produce single layer graphene in large area. Various synthesis parameters such as carbon source, substrate and temperature used have been

demonstrated to results in graphene.[20, 37-38] However, the requirement of transfer to suitable substrates and the high temperature deter the use of this technique in viable application processes.

Alternatively, modified Hummers' method successfully produced large quantity of graphene oxide sheets via exfoliation of graphite oxide.[21-22] This synthesis method is highly preferred as the single layer graphene oxide sheets obtained is low cost, high yield and solution processable. The produced GO sheets are well-dispersed in water because of existence of carboxylic acid, hydroxide and epoxide on the surface.[39] GO sheets are then can be reduced to obtain conductive reduced graphene oxide (rGO) sheets. Conductivity of rGO is improved as amount of reduction is increased. Reduction of graphene oxide has also been studied extensively by using various chemical reduction agents,[16, 21, 40-41] electrochemical reduction,[42-43] thermal treatment,[44] and photochemical[45] or photo-thermal treatment.[46] Hydrazine vapor is most commonly used reduction agent due to its dry, low temperature and simple reduction process. The resulted rGO is popular as an alternative material for graphene due to its high yield and facile process.

2.2 Carbon Nanoscrolls/ Graphene Scrolls

Recently, new graphene architecture in the form of scroll or known as carbon nanoscroll or graphene scroll has been reported. This scroll is made from scrolling of graphene sheet into a tube which results in a similar structure as CNT (as shown in Figure 2 - 1). However, in contrast to CNT which is enclosed tube, graphene scroll has exposed interlayer in which various intercalants can be inserted.

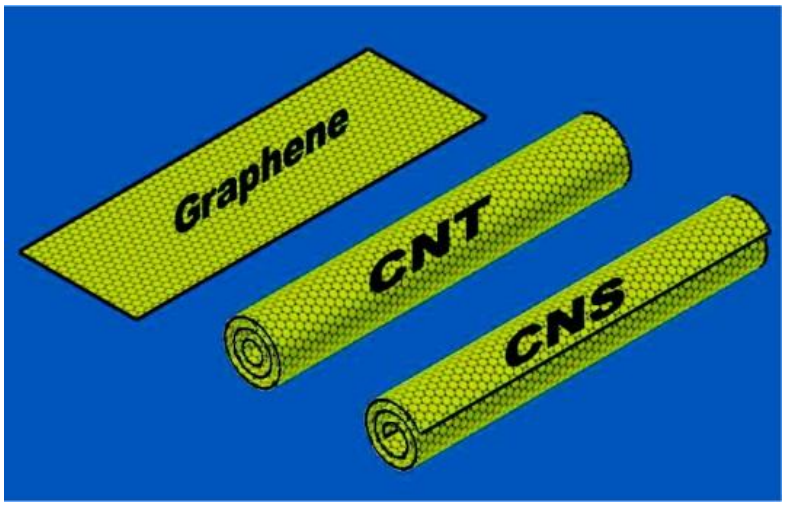

Figure 2 - 1. Representation of two dimensional graphene sheet, one dimensional carbon nanotube (CNT) and carbon nanoscroll (CNS) structure. Reprinted with permission from American Chemical Society.[47] Copyright 2009 American Chemical Society.

2.2.1 Fabrication of Carbon Nanoscroll/ Graphene Scroll

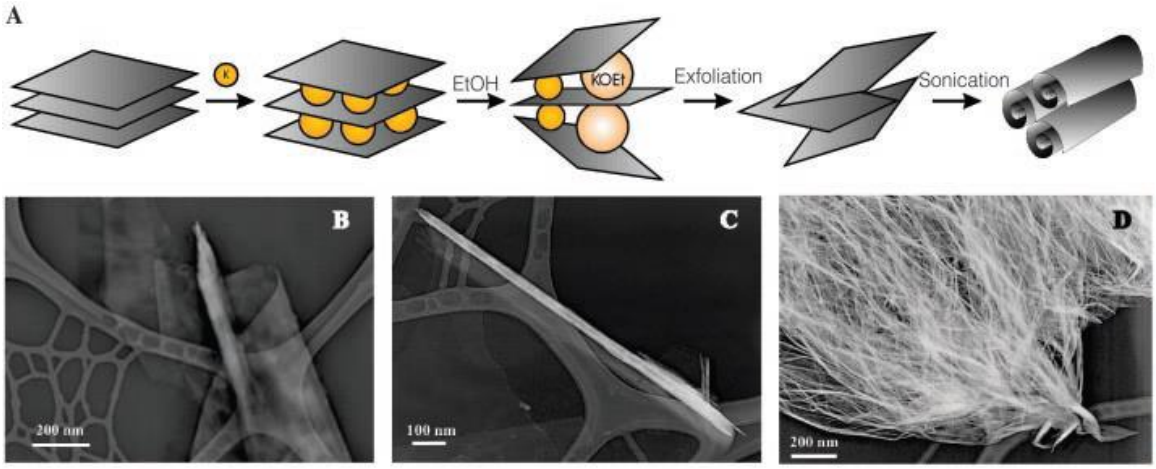

Figure 2 - 2. (A) Carbon nanoscroll (CNS) fabrication scheme. TEM images of (B) partially scrolled carbon nanoscroll (C) single carbon nanoscroll with open ends (D) bundled of carbon nanoscrolls. Reprinted with permission of The American Association for the Advancement of Science.[48]

First report on the production of carbon nanoscroll (CNS) is achieved by intercalation of graphite by KC_8 followed by dispersion of graphitic sheets in ethanol and sonication to form nanoscroll as observed in Figure 2 - 2.[48] Using high energy sonication, over 80% of graphitic sheets are transformed into CNS with average diameter of 40 nm. Following this experimental result, a few theoretical works has highlighted the importance of carbon nanoscroll/ graphene scroll.[49-52] Molecular dynamics simulation has shown that the scrolling of graphene sheet is energy assisted but grown in stability due to van der Waals interaction between interlayer graphene surfaces as it scrolls. CNS radius is also simulated to be affected by charge density and therefore demonstrated its potential as nanomechanical actuator.[49]

Alkali metal such as lithium is inserted into interlayer of CNS and therefore adjusts the interlayer distance accordingly. Theoretical calculation with density functional level of theory and classical Monte Carlo simulations, it is shown that interlayer distance of 7 Å resulted in 3 wt% of hydrogen absorption at ambient atmosphere.[50] CNS potential as hydrogen storage is also demonstrated with Monte Carlo simulations in which 5.5 wt% hydrogen storage capacity with interlayer distance of 6.4 Å.[52] First principle calculation is used to study the electronic property of CNS. Similar to CNT, chirality of CNS is the determining factor of its conductivity. Zigzag and armchair nanoscrolls are found to be small gap semiconductors and semi metallic/ metallic materials, respectively.[51]

CNS/GO scroll still exhibits inherent properties of GO sheets used as the main building block, such as high electrical conductivity and surface area with variations due to its architecture. As an example, GO scroll's specific capacitance is higher than GO sheet's. GO scroll fabricated via microexplosion method shows specific capacitance of 162.2 F/g at

the current density of 1 A/g, meanwhile, GO sheet showed specific capacitance of 110 F/g. GO scroll has scrolled structure with open ends to interact with electrolyte and form double electric layer within layers which then improved the properties.[53]

More interests in production of carbon nanoscroll/ graphene scroll have also been reported. High quality CNS is produced by using isopropyl alcohol solution to scroll mechanically exfoliated single layer graphene sheet. The resulting CNS based device has high current density of up to 5×10^7 A/cm^2.[47] Even though the prepared CNS is characterized with no defect, this technique has very low yield due to the use of mechanically exfoliated graphene. The successful scrolling of mechanically exfoliated graphene is also limited by graphene shapes and layer number.

Other techniques to produce carbon nanoscroll/ graphene scroll has been demonstrated such as Langmuir-Blodgett compression of octadecylamine (ODA) functionalized GO sheets,[54] microwave-assisted scrolling in liquid nitrogen,[55] intercalation of graphite followed by ultrasonication,[56-57] CNT-templated scroll,[58] and ruptured CVD graphene sheet.[59] GO sheets are first functionalized with ODA, spread onto water phase in Langmuir-Blodgett (LB) trough and left for 6 h to allow evaporation of toluene as solvent.[54] Compression of LB barrier results in loose-dense packed CNS. The prepared CNS are bundled hollow tube which is made of several combined ODA-GO sheets. Microwave irradiation of graphite in liquid nitrogen also reported to result in CNS.[55] Intercalation agents such as HNO_3[56] and MnO_2[57] are also used to intercalate graphite and produce graphene scroll after sonication. Due to the high energy process, impurities and defects are introduced on carbon nanoscroll/graphene scroll. Aminated MWCNT is also used as template to produce CNS via wet chemical synthesis in which GO

sheet wrap around MWCNT via covalent bond.[58] CVD graphene can also be scrolled during transfer process which used polymer.[59] Tearing of graphene during transfer process or polymer removal followed by drying resulted in formation of either straight or curvy graphene scroll. However, this method is not controllable.

2.2.2 Introduction to Molecular Combing

Molecular combing is first reported to align and stretch DNA molecules on silanized substrates.[60] In the early report, 5 μL of λ DNA solution is sandwiched between the silanized glass coverslip and untreated glass coverslip. λ DNA is then stretched during solvent evaporation as schematically shown in Figure 2 - 3. Molecular combing of DNA molecules mechanism is thought to occur in two steps: first, absorption of DNA molecules extremity (or extremities) on hydrophobic surface; two, stretching of DNA molecules by receding solvent/water meniscus. The unzipping of DNA double helix at extremity (or extremities) exposed its hydrophobic core which in turn binds onto hydrophobic surface via hydrophobic interaction. DNA molecules are then immobilized on the surface at one (or two) end(s) and pulled by receding solvent\water meniscus. However, the detailed mechanism of stretching due to molecular combing has not been confirmed yet.

Following the report by Bensimon *et al.* at 1994,[60] there have been more reports on the improvement of molecular combing technique. Mechanical movement of solvent/solution meniscus can result in faster combing with reliable stretching and alignment of DNA molecules. Briefly, a motor-drive is attached to a glass coverslip which in turn is placed at 45^{o} angle to silanized glass slide. A 2 - 5 μL of DNA solution is then deposited in between a glass slide and a glass coverslip's edge. As glass coverslip is pulled

by motor-drive at a speed of 3 cm/min, stretched and aligned DNA molecules are left on silanized glass slide.[61] A dynamic molecular combing which is developed based on Langmuir-Blodgett thin film deposition technique is also described. Silanized substrates are immersed onto DNA solution at pH = 5.5 for 5 min and pulled upwards out of the solution at a constant speed.[62] Similarly, DNA is anchored on silanized substrate and the downward force provided by solution meniscus enable the stretching of DNA molecules parallel to the pulling direction. However, this technique requires larger volume of DNA solution.

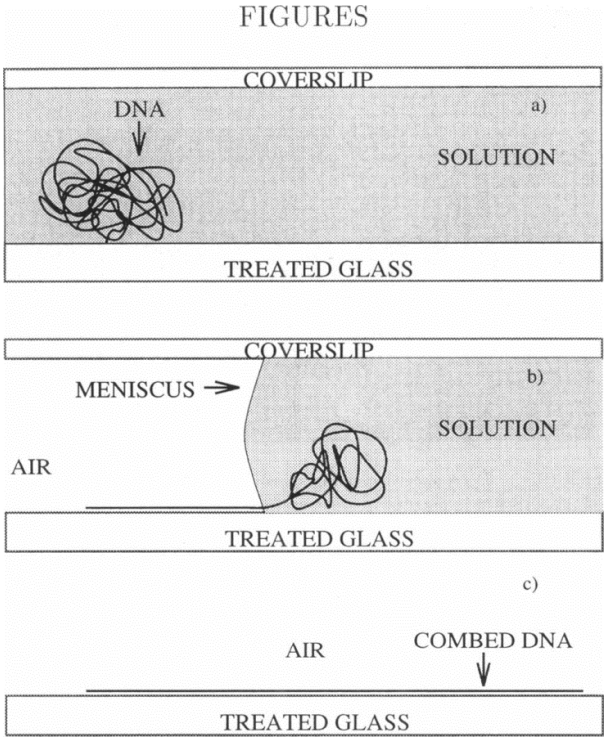

Figure 2 - 3. Schematic diagram of molecular combing process. (A) DNA molecule on treated glass slide. (B) DNA molecule binds to substrate at one extremity and stretches along solvent receding direction. (C) Stretched DNA molecule after combing. Reprinted with permission from Elsevier.[63]

DNA molecules can be stretched on mica surface by nitrogen gas flow which forced DNA solution to move in the direction of gas flow.[64-65] However, the distance, direction and angle of gas stream to substrate will affect the stretching of DNA molecules. Another approach of molecular combing is performed by utilizing gravitational force. A drop of DNA solution is positioned on treated substrates and then tilted up to 80^{o} to let DNA solution flow downwards.[66-67] Molecular combing can also be performed by using pipette to draw DNA solution from substrate surface.[68-69] The movement of the solvent meniscus results in stretching of DNA molecules.

2.3 Surface Wettability

Substrate's surface property such as wettability displays significant role in various chemical, biological and physical processes. Hydrophilic surface which has better wettability is a preferable surface to minimize amyloid fibril nucleation and growth.[70] In addition, small and short fibrils were formed on hydrophilic surface while amorphous globular aggregates were observed on hydrophobic substrates.[71] The shape formation of silver nanostructures is guided by reaction flask wettability. Lower contact angle surface resulted in silver nanowire, while higher contact angle surface resulted in assembly of nanospheres such as cube, star, belt, and microsphere.[72]

2.3.1 Patterned Hydrophilic-Hydrophobic Self-Assembled Monolayers

Patterned hydrophilic-hydrophobic surface is often utilized as templates to control deposition or placement of various materials. Controlled surface wettabillity can also enhanced quality of molecules printing technique by increasing wettability contrast

between hydrophilic and hydrophobic patterned areas.[73] Patterned hydrophilic and hydrophobic alkanethiols on gold surface has been reported for fabrication of small DNA arrays.[74] In another instance, hydrophilic polymer surrounded by superhydrophobic polymer enabled confinement of cell lines and therefore allowed co-culturing of multiple cell types at the same time without cross-talk.[75] Patterned hydrophobic silane on hydrophilic glass substrate is also demonstrated as selective deposition technique in which nickel particle is exclusively deposited on hydrophilic area.[76]

Fabrication of patterned hydrophilic-hydrophobic surface using self-assembled monolayers (SAMs) has gained extensive interest mainly due to its ease of fabrication and the availability of various surface functionalities.[77] The patterned hydrophilic-hydrophobic SAMs are able to direct the assembly of different materials such as polymer, magnetic particles, tungsten dioxide and CNT.[78-82] Patterned hydrophilic-hydrophobic SAMs are produced on gold substrates by micro-contact printing (μCP) of 16-mercaptohexadecanoic acid (MHA) as hydrophilic SAMs followed by passivation of non-printed area with hexadecanethiol (HDT) as hydrophobic SAMs. The patterned substrates are cooled below the dew point to form water droplets on hydrophilic region and then dipped into polystyrene in chloroform solution. Polystyrene rings are formed as water and chloroform evaporates. Polystyrene rings formation on gold substrates are directed by combination of water condensation on hydrophilic region as well as surface directed and concentration controlled dewetting process.[78]

Assembly of metal particles such as magnetic particles [79-80] and tungsten oxide[82] can be directed as well by patterned hydrophobic-hydrophilic SAMs. HDT SAMs is printed on gold substrates by μCP and dipped on hydrophilic thiol solution. Iron oxides are

selectively deposited on hydrophilic region despite of functionalities of hydrophilic SAMs.[79] Another patterning of octadecyltrichlorosilane SAMs on hydrophilic SiO_2/Si is performed through μCP. Magnetic nanoparticles such as $MgFe_2O_4$ or $NiFe_2O_4$ arrays are selectively formed on the hydrophilic region after solvent evaporation.[80] 11-mercaptoundecanol and octadecanethiol (ODT) are used as hydrophilic and hydrophobic SAMs respectively, which are patterned with PDMS stamp casted from polystyrene microspheres. Tungsten oxide (WO_3) dot array is left on hydrophilic region via sol-gel transition.[82]

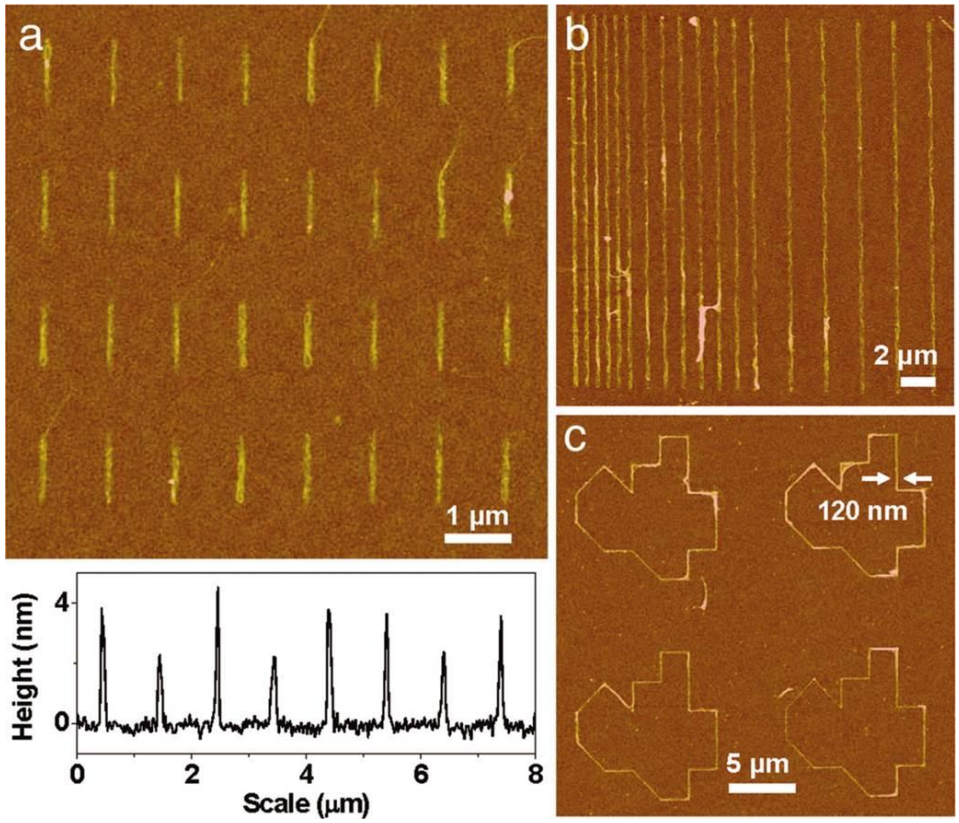

Figure 2 - 4. AFM images of single walled carbon nanotube (SWCNT) arrays. (A-B) Aligned SWCNT on MHA lines templates. (C) Precise positioning of SWCNT on arbitrary MHA templates. Reprinted with permission from National Academy of Sciences.[81] Copyright (2006) National Academy of Sciences, U.S.A.

Patterned hydrophobic and hydrophilic SAMs on gold substrates are also reported to direct the assembly of single wall carbon nanotube (SWCNT).[81] Dip-pen nanolithography is used to generate MHA pattern on gold substrate and the non-patterned area is covered with ODT SAMs. CNT solution in 1,2-dichlorobenzene only wets hydrophilic region and hence led to selective CNT assembly due to van der Waals attraction between CNT and MHA (see Figure 2 - 4). As CNT is much longer than the MHA patterned area, CNT is preferably assembled in the perimeter of MHA patterned region to maximize contact area with MHA and minimize CNT bending at the same time. Surface functionalities of MHA and passivation layer of ODT SAMs are proven to be essential in precise assembly of CNT around MHA circumference. CNT architectures consist of CNT rings, line arrays, filtration membranes and various architectures defined by patterned MHA shape has been demonstrated.

2.3.2 Micro-contact Printing

Micro-contact printing (μCP) is generally used to fabricate pattern of various SAMs on different types of substrates over large area successfully. Micro-contact printing has shown its flexibility to form various patterned SAMs with complex micrometer sized features. It is first introduced by Kumar *et al.* in which alkanethiol ink is stamped on gold substrate with elastomeric stamp.[83] Features on elastomeric stamp is designed accordingly on silicon (Si) master which is fabricated by common photolithography technique. A general procedure of μCP is shown in Figure 2 - 5. Typically, silicone elastomer and its curing agent is mixed thoroughly in 10:1 ratio (w:w) and poured over Si master. After degassing, the elastomer is cured and peeled away from Si master. The resulting elastomeric

stamp is inked with desired molecules, blown dried and stamped on desired substrates. The desired ink molecules will be transferred on substrates according to the protruding features on PDMS elastomeric stamp.

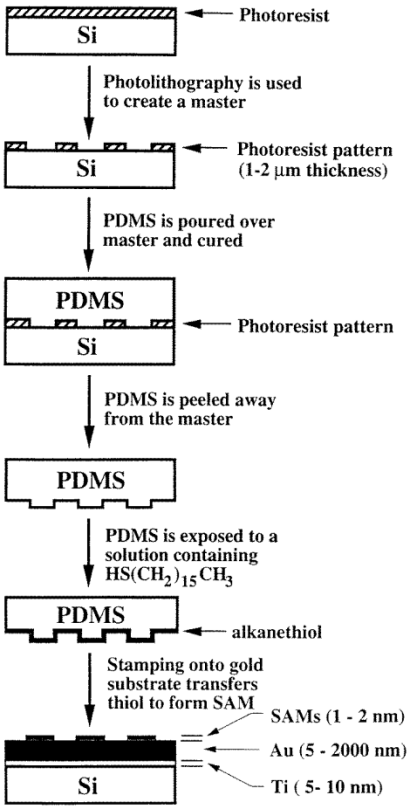

Figure 2 - 5. Schematic diagram of micro-contact printing (μCP) procedure. ©IOP Publishing. Reproduced by permission from ION Publishing.[84] All rights reserved.

2.4 Transparent and Flexible Electronics

Owing to its excellent electrical properties, graphene has been considered as active material for electronics application. Future of electronics has started to migrate towards transparent and flexible devices. Graphene has also been demonstrated as active material or electrode for transparent and flexible electronic devices due to its high transparency and

excellent conductivity.[37, 85-87] Big scale production of graphene via chemical vapor deposition are reported and transferred on flexible substrate to demonstrate its potential in flexible electronics.[37, 87] Low sheet resistance of ~230 - 280 Ω/sq coupled with optical transmittance of ~70 - 80% are achieved. Furthermore, as electrode, CVD graphene exhibited comparable performance to indium tin oxide (ITO) electrode. In addition, graphene oxide reduced via thermal annealing[85] and photoreduction[86] were used as transparent electrode in photovoltaic devices. Both devices exhibit higher sheet resistance of ~700 Ω/sq and lower optical transmittance of ~40% compared to CVD graphene. Generally, sheet resistance of rGO can be improved by using thicker film but it is compensated on lower transparency.

2.4.1 Graphene Mesh Electrode

Graphene in mesh or network architecture has been recently introduced. Graphene woven fabrics (GWF) which is fabricated by chemical vapor deposition at temperature of 1000 ºC with woven copper mesh as template.[88] GWF which consist of woven graphene micro-ribbons of 100 μm width are produced after copper mesh is etched. GWF on PDMS films are reported as strain or touch sensors device due to its sensitivity towards strain which resulted in resistance change.[89-91] Supercapacitor electrode based on GWF has also been recently reported. GWF is deposited on various substrates with attached silver wire, two of these identical GWF and Poly (vinyl alcohol) (PVA)-H_3PO_4 polymer gel electrolyte constructed the complete supercapacitor. Excellent supercapacitor performance is obtained with area specific capacitance of up to 267 F/g with 1 - 7 nm thick GWF electrode.[92] The flexibility of GWF enabled this electrode to be folded and twisted.

Another graphene in mesh or network architecture is reported as graphene mesh in planar configuration for transparent electrode.[93] The graphene mesh is produced via photolithography combined with oxygen plasma. The schematic diagram illustrating the fabrication process of graphene mesh is shown on Figure 2 - 6. GO solution produced by modified Hummers' method is spin-coated on quartz substrate and further annealed at 950 ^{o}C to restore its conductivity. Photoresist is spin-coated on rGO film, exposed to UV light under photolithographic mask, developed, and exposed to oxygen plasma followed by removal of photoresist. The produced rGO film (thickness of ~100 nm) which are not covered by photoresist are etched away during oxygen plasma. Therefore, rGO film pattern is determined and controlled by the photolithographic mask.

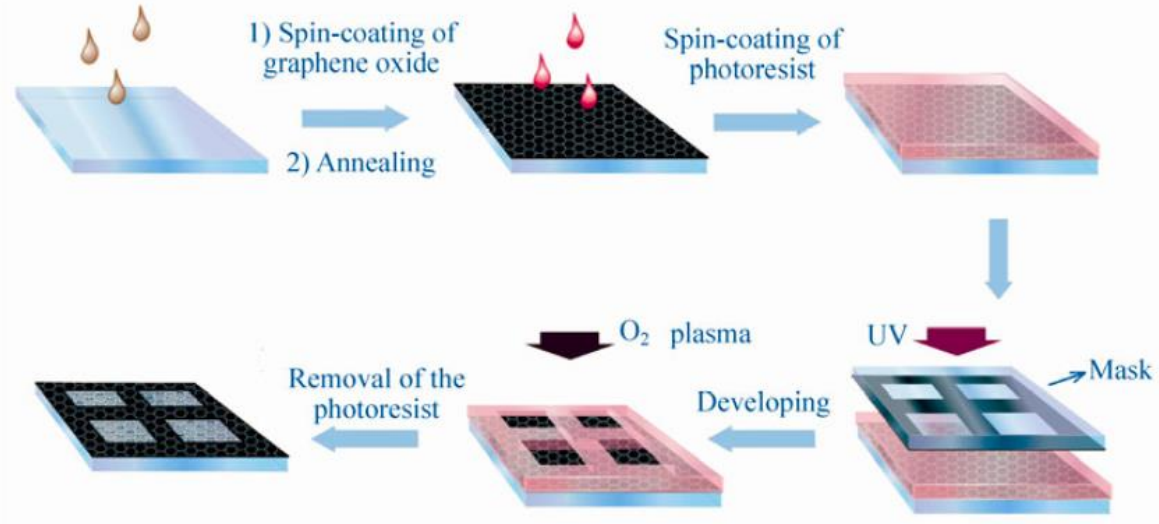

Figure 2 - 6. Schematic diagram of graphene oxide mesh fabrication method. Reproduced with permission from Springer.[93]

The rGO mesh pattern with line width of 10 μm and period of 50 μm is obtained with maximum transparency of 65% and sheet resistance of 0.7 kΩ/sq. Transparency and

conductivity of rGO mesh is highly dependent on oxygen plasma etching time in which transparency/depth of etch pit increases as time increases. rGO mesh is used as transparent electrodes in organic photovoltaic and is shown to have better performance compared to analogous cells with rGO film based electrode.[93]

2.4.2 Graphene Transfer

Two-dimensional materials such as graphene currently require transfer step to integrate them into viable functional applications. There are many reports on transfer techniques such as transfer printing with PDMS stamp,[94] lift off through etching[95-96] and peel off with PMMA support.[97] These transfer techniques which has been demonstrated previously suffered from a few drawbacks such as selective transfer due to interface adhesion force, etchant-induced defects on 2D material and incomplete polymer removal or harsh environment condition during polymer removal process.

Transfer by etching of underlying substrate (Cu or SiO_2) are commonly used to lift off nanomaterial such as graphene and CNT. PMMA as support film is spin-coated on substrate and followed by etching of Cu or SiO_2 layer to release PMMA-nanomaterial film. PMMA-nanomaterial film is transported on target substrate and PMMA is dissolved away with acetone leaving nanomaterial on target substrate.[95-96]

Simple transfer printing of various materials such as HOPG and mica utilizing PDMS stamp are demonstrated on variety of substrates. The transfer of materials is achieved through switching of adhesion and release of materials to and from elastomeric PDMS stamp which can be controlled kinetically. Fast peel off movement (~10 cm/s) resulted in adhesion of materials from a substrate to PDMS stamp. In the other hand, slow

peel off movement (~1 mm/s) resulted in release of materials from PDMS stamp onto desired substrate.[94]

Another transfer technique via Poly (methyl methacrylate) (PMMA)-mediated transfer is reported. PMMA solution in spin-coated on a substrate with deposited nanomaterials and then hydrolyzed it in basic solution to detach it from substrate. PMMA-nanomaterial film is attached on desired substrate and annealed at 50 ^{o}C for 5 min. PMMA as carrier film is removed with acetone vapor or thermal annealing at 300 ^{o}C.[98]

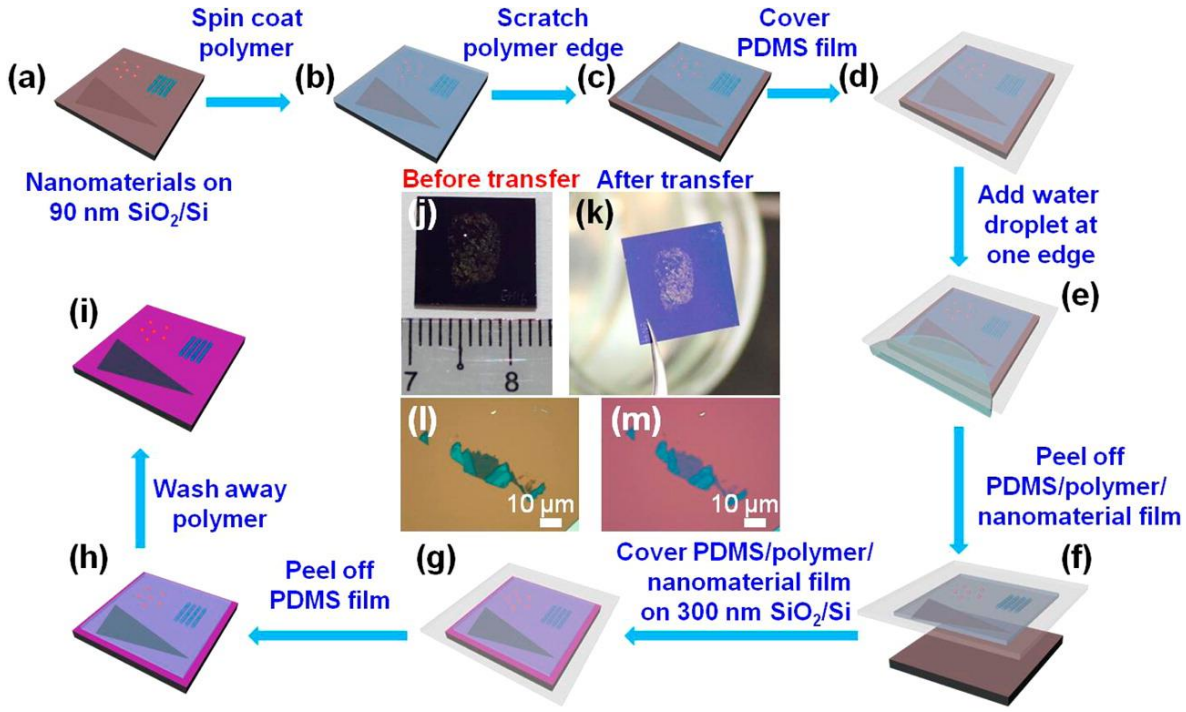

Figure 2 - 7. Schematic diagram of nanomaterials transfer technique. (A) Nanomaterials deposited on 90 nm SiO_2/Si (or initial substrate). (B) Polymer is spin-coated on the substrate containing nanomaterials. (C) Polymer is removed at the edges to expose the underlying substrate. (D) 1 - 2 mm thick PDMS film is brought into contact with polymer. (E-F) Water droplet is deposited on one edge of substrate to aid removal of PDMS-polymer-nanomaterials from substrate. (G) PDMS-polymer-nanomaterial is brought into contact with 300 nm SiO_2/Si (or target substrate). (H-I) PDMS film is detached from polymer and the polymer is dissolved in dichloromethane (DCM) at 50 ^oC to leave nanomaterials on the target substrate. Photographs of MoS_2 flakes taken (J) before transfer on 90 nm SiO_2/Si and (K) after transfer on 300 nm SiO_2/Si. Optical microscopy images of MoS_2 sheets (L) before and (M) after transfer. Reprinted with permission from American Chemical Society.[98] Copyright (2014) American Chemical Society.

Recently our group has reported a clean transfer technique which can be applied to various substrates to transfer nanomaterials in different dimensionalities including nanoparticle, nanowire and nanosheet.[98] Schematic representation of transfer technique is shown in Figure 2 - 7. The described transfer technique utilized polymer as carrier and PDMS film as support layer to transfer nanomaterials. Successful and reliable transfer with no polymer residues is achieved with no thermal annealing and etching process required.

Chapter 3:

Experimental Details

3.1 Chemicals and Materials

Silicon wafer with thermal oxide thickness of 300 nm (300 nm SiO_2/Si) was purchased from Bonda Technology Pte Ltd, Singapore. Microscope glass slides and glass coverslip used are from SAIL Brand, China and Paul Marienfeld GmbH & Co. KG, Germany respectively. Sulfuric acid (H_2SO_4, 95 - 97%) was purchased from Honeywell, USA. Hydrogen peroxide (H_2O_2, 30%) was procured from VWR, SG. Polydimethylsiloxane/Silicone elastomer kit (PDMS, Sylgard 184) was purchased from Dow Corning, USA. Poly (L-lactic acid) (PLLA, IV 2.38) was purchased from Bio Invigor Corporation, Taiwan. Hydrochloric acid (HCl, fuming, 37%), Potassium permanganate ($KMnO_4$, 99%), Potassium persulfate ($K_2S_2O_8$, 99%), Phosphorus pentoxide (P_2O_5, 98%), Hydrazine monohydrate (N_2H_4, 98%), Dichloromethane (DCM, 99.8%), Octadecyltrimethoxysilane (OTS, 90%), 1-Octadecanethiol (ODT, 98%), 11-Mercapto-1-undecanol (MUO, 99%), 4-Aminothiophenol (ATP, 97%), 16-Mercaptohexadecanoic acid (MHA, 99%) were from Sigma-Aldrich, USA. Ethanol (99%) was purchased from Merck Pte Ltd, Singapore, methanol (99.99%) was from Fisher Scientific, UK and toluene (anhydrous, 99.8%) was from Sigma-Aldrich, USA. Natural graphite (SP-1) was purchased from Bay Carbon (Bay City, MI). Ultrapure Milli-Q water with resistivity of 18.2 MΩ.cm (Milli-Q System, Millipore, USA) was used in all experiments. Chromium plated Tungsten rod (Cr, 99.99%) was from TED Pella, Inc., USA and gold wire (Au, 99.99%) was bought from

Goodfellow Corporation, USA. Silver conductive paste is obtained from RS Components, Singapore. NO_2 (2 or 5.8ppm in N_2) and N_2 (99.99%) gas were obtained from National Oxygen Pte Ltd, Singapore.

3.2 Synthesis of Graphene Oxide (GO) and Reduced Graphene Oxide (rGO)

3.2.1 Synthesis of GO

Large GO sheets were synthesized by modified Hummers' method with natural graphite (SP-1) as precursor.[22, 99] In short, 0.3 g graphite was added step-wise into an aqueous solution which contains H_2SO_4 (2.4 mL), $K_2S_2O_8$ (0.5 g) and P_2O_5 (0.5 g) and kept at temperature of 80 °C for 4.5 h. The product was pre-oxidized graphite which then washed with Milli-Q water and dried overnight at 50 ^oC, followed by addition of H_2SO_4 (12 mL) solution. While maintaining the mixture at below 0 ^oC, $KMnO_4$ (1.5 g) was added slowly. The reaction was allowed to continue for 2 hours before adding Milli-Q water (100 mL) to dilute the mixture. H_2O_2 (2 mL) was further added into the solution to react with excess $KMnO_4$. The resulting solution was purified first with HCl for 3 times and followed by Milli-Q water to reach pH~7.

3.2.2 Synthesis of rGO

Reduced graphene oxide (rGO) as the name implies, was obtained by reduction of graphene oxide. In this work, GO was reduced by hydrazine vapor and/or thermal annealing. Deposited GO on substrate were positioned along with 100 μL hydrazine in an aluminium covered glass petridish and heated at 70 ^oC overnight. Thermal annealing is performed in

quartz tube positioned within a furnace. Substrate containing GO is placed within quartz tube and purged with Ar gas for 5 min at 350 sccm after it is sealed. Annealing is performed in mixed gas of H_2 (150 sccm) and Ar (50 sccm) with ramp rate at 10 ^oC/min, and maintained at 200 ^oC for 5 h.

3.3 Synthesis of GO Scroll

3.3.1 Formation of Hydrophobic Substrates

3.3.1.1 Preparation of SiO_2/Si Substrate

Rectangular pieces of 300 nm SiO_2/Si wafer and glass slides in the size of 1 cm × 1.5 cm were immersed in solution of acetone and water (v/v = 1:1) and sonicated for 20 min. After thorough rinsing by Milli-Q water, the substrates were immersed into piranha solution which contained a combination of H_2SO_4 and H_2O_2 with 1:1 v/v ratio. The mixture was then brought to boil at 120 ^oC for 1 h. After 10 min cooling period, the substrates were washed with Milli-Q water thoroughly and blow dried with nitrogen gas. The substrates were always used within 2 weeks.

3.3.1.2 Thermal Evaporation of Gold-Coated SiO_2/Si

Gold-coated SiO_2/Si was prepared by thermal evaporation (Quantum Vac Thermal Evaporator, Elite Engineer) with vacuum level below 5×10^{-6} mbar. 5 nm of chromium (Cr) was first deposited on substrates at a rate of 0.2 Å/s followed by 50 nm of Au at a rate of 0.3 Å/s. Vacuum chambers were allowed to be cooled for minimum of 2 hours before substrates were withdrawn. Gold-coated SiO_2/Si was used after 1 day exposure in ambient atmosphere which was referred as aged gold-coated SiO_2/Si.

3.3.1.3 Functionalization of Octadecyltrimethoxysilane (OTS) on SiO_2/Si

OTS-SiO_2/Si was prepared by immersing substrates on 1% OTS in anhydrous toluene solution for 1 day at 50 ^oC. The substrates were washed thoroughly with ethanol followed by Milli-Q water and blown dried with nitrogen gas.

3.3.1.4 Spin-Coating of Poly (L-Lactic Acid) (PLLA) on Glass Slides

Glass slides were prepared as described in section 3.3.1.1. Next, 3 wt% PLLA was first dissolved in DCM under magnetic stirring for minimum 3 h. PLLA solution was spin-coated on glass slides at 3,000 - 3,500 rpm and allowed to dry in ambient atmosphere overnight.

3.3.1.5 Fabrication of Polydimethylsiloxane (PDMS) Film

Sylgard 184 elastomer and curing agent (w/w = 1:1) were carefully mixed for 30 min and degassed at room temperature until clear mixture was observed. The mixture was then poured onto a clean petri dish, degassed and cured at 70 ^oC for 12 h.

3.3.2 Molecular Combing of GO

Molecular combing technique was executed on hydrophobic substrate to produce GO scroll. Hydrophobic substrates such as Au-coated SiO_2/Si, OTS-SiO_2/Si, PLLA or PDMS were placed over a filter/absorbent paper. A clean glass coverslip (22 × 22 mm^2) was positioned at one end of the substrates at angle of 45^o to hydrophobic substrates with 10 - 50 µL GO solution placed in between them. Glass coverslip were then dragged over towards the other end of substrates with speed of 1 - 3 mm/s (Figure 3 - 1). Excess GO solution was then absorbed by filter/absorbent paper.

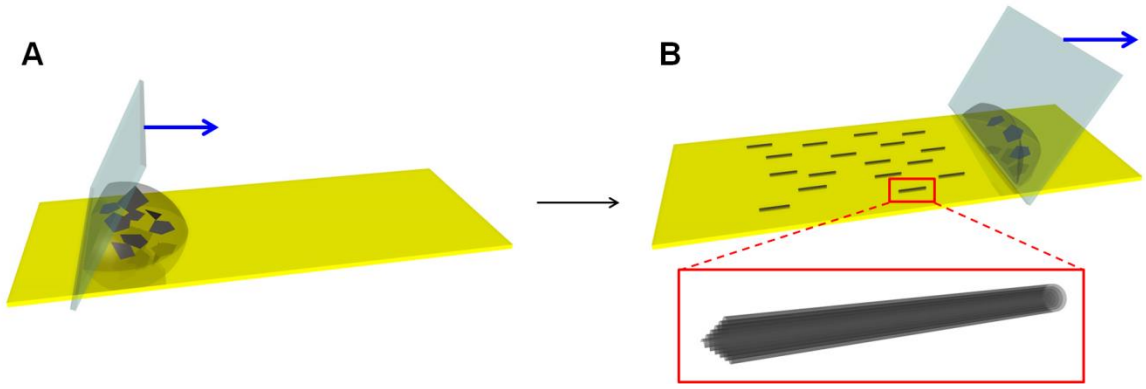

Figure 3 - 1. Schematic representation of molecular combing of GO sheets in solution on a gold-coated SiO_2/Si substrates. (A) A coverslip was positioned at an angle to substrate and droplet of GO sheets in water solution is placed. (B) Coverslip is pulled onto the other end and GO scrolls formed as water meniscus receded.[18] Reprinted with permission from John Wiley and Sons.

3.4 Synthesis of other GO Architectures

Other GO architectures were fabricated by utilizing alternating hydrophilic and hydrophobic region on the substrate. These regions were generated by patterning of self-assembled monolayers as described below.

3.4.1 Generation of Hydrophilic-Hydrophobic Pattern on Substrates

3.4.1.1 Fabrication of PDMS Stamp

Similar to description on section 3.3.1.5, Sylgard 184 elastomer and its curing agent are mixed in 1:1 (w/w) ratio and were carefully mixed for 30 min. The mixture was degassed at room temperature until clear mixture was observed. PDMS mixture was then poured over on Silicon masters which were placed in a petri dish. Silicon master or templates which

contained various topographic patterns were fabricated beforehand by photolithography technique. The mixture were degassed for the second time for 1 h and then cured at 70 ^{o}C for 12 h.[100-101] Cured PDMS was peeled off from the master/template and used as stamp.

3.4.1.2 Printing of Hydrophilic Self-Assembled Monolayers

Self-assembled monolayers pattern were generated on gold-coated SiO_2/Si by micro-contact printing (μCP). Alkanethiols such as MHA, ATP, MUO (0.5 mg/mL) and ODT (1 mg/mL) were mixed in ethanol (99 %) and dissolved by sonication for 30 s. These alkanethiols were prepared immediately before they were to be used as inking molecules. Prepared PDMS stamp with certain pattern was immersed in MHA solution for 1 min, or in ATP or MUO solution for 5 min as hydrophilic region. Subsequently, the inked PDMS stamp was blown dried for 30 s with nitrogen gas. Inked PDMS stamps were then contacted with gold-coated SiO_2/Si for 30 s. PDMS stamp can then be re-used for printing. Consequently, the MHA/ATP/MUO stamped gold-coated SiO_2/Si was immersed into ODT for 10 min to passivate the unstamped region and act as hydrophobic region.

To produce dot or line patterned MHA/ATP/MUO, PDMS stamp with feature of 2, 5, 10, and 20 μm were utilized. These patterned substrates will be labeled as dotted or lined MHA/ATP/MUO - ODT patterned substrates. In the other hand, cross patterned MHA were produced by printing inked PDMS stamp with line feature in both vertical and horizontal direction. Note that printed SAMs with *x* μm - *y* μm dimension refers to feature size of *x* μm and the distance between the feature is *y* μm.

3.4.2 Molecular Combing of GO

In order to produce other GO architectures, molecular combing of GO sheet in aqueous solution was performed on dot, line or cross patterned MHA/ATP/MUO substrates. On dotted or crossed MHA/ATP/MUO - ODT patterned substrates, molecular combing was performed as described in section 3.3.2. On lined MHA - ODT patterned substrates, molecular combing of GO were performed with cover slip movement along the lined MHA - ODT patterned substrates. The schematic diagram of molecular combing of GO sheets in aqueous solution on hydrophilic-hydrophobic patterned substrates is shown on Figure 3 - 2.

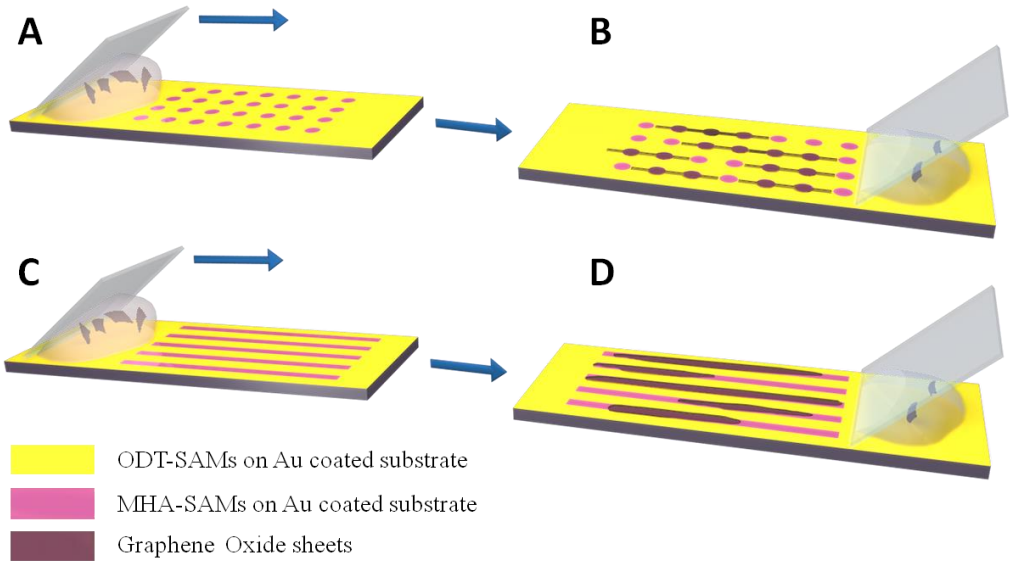

Figure 3 - 2. Schematic representation of molecular combing process of GO sheets in solution on MHA-ODT patterned gold-coated SiO_2/Si. (A) Before molecular combing and (B) after molecular combing of GO sheets in solution on dotted MHA-ODT patterns to form beaded GO string. (C) Before molecular combing and (D) after molecular combing of GO sheets in solution on lined MHA-ODT patterns.[102] Reprinted with permission from John Wiley and Sons.

3.5 Synthesis of Graphene Oxide (GO) Scroll Mesh

Graphene oxide (GO) scroll mesh is fabricated through combination of molecular combing to produce GO scroll and transfer of high density GO scroll to form mesh configuration. The detailed procedure will be described below.

3.5.1 Molecular Combing and Transfer of GO Scroll

Molecular combing of GO sheets in aqueous solution to obtain GO scroll is executed as described in section 3.3. In short, GO solution is deposited on one side of hydrophobic substrate and pulled to the other side of the substrate with glass coverslip. Concentration of GO sheets in aqueous solution determines the density of GO scrolls fabricated on hydrophobic substrate. High density GO scrolls can be obtained at GO concentration of ~1.5 mg/mL. In order to result in mesh/network configuration, GO scrolls in horizontal and vertical directions are fabricated on hydrophobic substrates.

First, molecular combing of GO is executed in horizontal direction on one OTS-SiO_2/Si resulting in horizontal GO scrolls as shown in Figure 3 - 3A. A second molecular combing of GO is executed in vertical direction on another OTS-SiO_2/Si resulting in vertical GO scrolls as shown in Figure 3 - 3B. Vertical GO scrolls is then transferred on top of horizontal GO scrolls as described on section 2.4.2 (or Figure 2 - 7). Poly (L-Lactic Acid) (PLLA) is spin-coated on substrate containing vertical GO scrolls. PDMS is used to support PLLA film carrying vertical GO scrolls and brought to contact on substrate containing horizontal GO scrolls (Figure 3 - 3C). PLLA is dissolved away with DCM at 50 ^{o}C after PDMS is removed. After transfer is completed, GO scroll mesh is formed on the substrate

as shown in Figure 3 - 3D. GO scroll mesh can then be transferred on other substrates such as quartz or polyethylene terephthalate (PET) (Figure 3 - 3E).

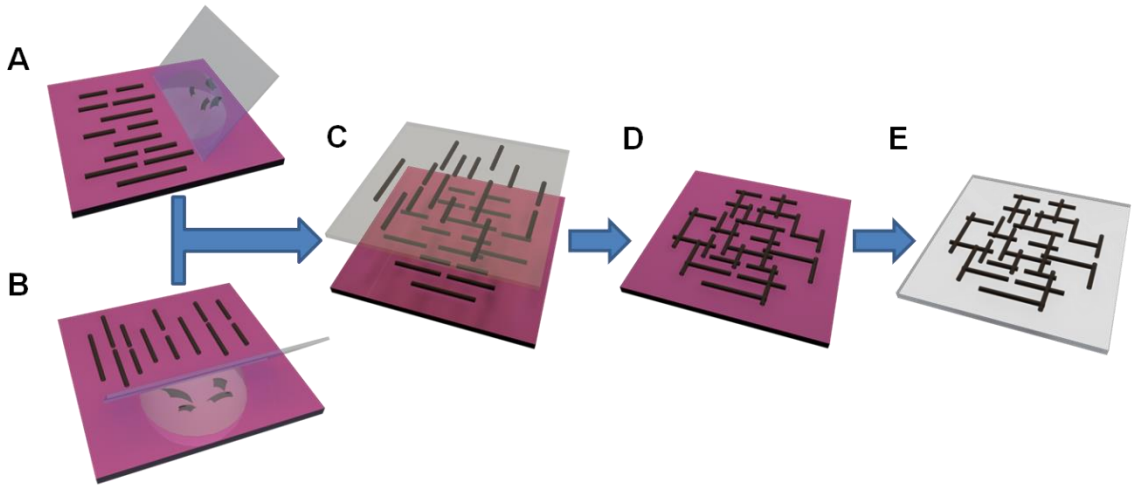

Figure 3 - 3. Schematic diagram of graphene oxide (GO) scroll mesh fabrication process. Molecular combing of GO sheets in (A) horizontal direction and (B) vertical direction on OTS-SiO_2/Si substrate. (C) PLLA film with vertical GO scrolls is transferred on horizontal GO scrolls. (D) GO scroll mesh formation after PLLA removal. (E) GO scroll mesh can be transferred on other transparent and flexible substrates.

3.5.2 Reduction of GO Scroll Mesh

The fabricated GO scroll mesh is then reduced to rGO scroll mesh in order to restore its conductivity. Reduction of GO scroll mesh is performed in two different methods. One method is in which GO scroll mesh on substrate is reduced with hydrazine vapor. GO scroll mesh on a substrate is placed on glass petridish along with 100 µL hydrazine and left overnight at 70 ^{o}C. Another method to reduce GO scroll mesh is a combination of hydrazine vapor and thermal annealing. GO scroll mesh is first reduced with hydrazine at 70 ^{o}C

overnight followed by thermal annealing to increase its conductivity. GO scroll mesh on substrate is placed inside quartz tube and sealed tightly. Thermal annealing is performed in a mixture of H_2 (150 sccm) and Ar (50 sccm) gas at 200 ^oC for 5 h.

3.5.3 Fabrication of GO Scroll Mesh Based Flexible Device

After fabrication of GO scroll mesh on OTS-SiO_2/Si, GO scroll mesh can be transferred on transparent and/or flexible substrates. GO scroll mesh is transferred on PET substrate (thickness 0.1 mm) as described in section 3.5.1 and processed it into rGO scroll mesh by reduction as described in section 3.5.2. Silver conductive paint (RS components) are applied on both ends of rGO scroll mesh as electrodes. Silver paint is allowed to dry at room temperature overnight before any electrical measurement is made.

3.6 Characterization Methods

Various characterization techniques were performed to analyze the fabricated GO scroll, other GO architectures and GO scroll mesh.

3.6.1 Optical Microscopy (OM)

Optical microscope (Eclipse LV100D, Nikon) were used to capture all fabricated GO scroll, other GO architectures and GO scroll mesh optical images with a digital camera control unit (DS-U3) and its camera head (DS-Fi1).

3.6.2 Scanning Electron Microscopy (SEM)

Scanning Electron Microscopy (SEM, JEOL JSM-6360) was performed to characterize fabricated GO scroll and other GO architectures. Accelerating voltage of 3 - 5 kV was used in imaging. No additional sample preparation is needed for SEM imaging.

3.6.3 Atomic Force Microscopy (AFM)

Atomic Force Microscopy (AFM, Bruker Dimension ICON) characterization was carried out to image all samples in air with tapping mode. It was equipped with Nanoscope V controller and scanner with scanning size of 90 × 90 μm^2. AFM tips with Silicon cantilevers with resonance frequency of 300 kHz and spring constant of 40 N/m (Tap 300Al-G, Budget Sensors, Innovative Solutions Bulgaria Ltd) or 42 N/m (OTESPA, Bruker AXS Pte Ltd). Scan rate of 1 - 2 Hz and resolution of 512 × 512 pixels were used to capture all AFM images.

3.6.4 Transmission Electron Microscopy (TEM)

Transmission Electron Microscopy (TEM) characterization was carried out with JEOL JEM 2100F at an accelerating voltage of 200 kV. TEM samples were prepared by transferring GO scroll or other architectures on TEM grid with holey carbon support. The transfer process was performed as described in detail by Li, *et al.*[98] In short, PLLA was spin-coated at 3,500 rpm onto gold-coated substrates containing GO scroll or other GO architectures. After drying at room temperature overnight, PLLA film was detached from substrate and moved to TEM grid by using PDMS film as support. After PDMS was

removed and PLLA was dissolved in DCM at 50 ºC, GO scrolls or other architectures were left on holey carbon TEM grid.

3.6.5 Raman Spectroscopy

Raman spectroscopy and mapping was carried out to analyze the fabricated GO scrolls, other GO architectures and GO scroll mesh. WITec α300S.R. (WITec Instrument Corp, Germany) with 488 nm laser was used at room temperature during characterization process. Raman spectrum of Si wafer at 520 cm^{-1} was taken as reference for calibration spectrum.

3.6.6 Gas Sensing Measurement

The produced GO scroll and beaded GO string were reduced with hydrazine vapor as described in section 3.2.2 to increase its conductivity. Single rGO scroll and/or beaded rGO string were used to fabricate gas sensing device. Athene 200-mesh TEM grid was used as a mask during thermal evaporation to create gold source and drain electrodes. Thermal evaporation was performed as described in section 3.3.1.2.

Gas sensing measurement was then carried out in a home-made gas sensing system in a glove box at room temperature. Electrical measurement was measured with Keithley 4200 semiconductor characterization system. The fabricated devices were stabilized in N_2 gas for 1 h before exposure to NO_2 toxic gas. The real-time current change was monitored as NO_2 gas was injected into glove box. Concentration of NO_2 was adjusted by controlling the flow meter and further dilution with N_2 gas.

3.6.7 UV-Vis Transmittance

GO/rGO scroll mesh is transferred on glass slide before its' transparency is measured by UV-Vis-NIR spectrometer (Cary 5000, Agilent Technologies). Transmittance is measured over a wide range of wavelength from 300 to 3300 nm. Blank glass slide is used as reference.

3.6.8 Four-Point Probe

Sheet resistance of rGO scroll mesh is measured using four point probe (SYS-301, Signatone). Sourcemeter and multimeter used are Keithley 224 and Keithley 2000 respectively. Sheet resistance reading is averaged over measurements at 10 different locations.

Chapter 4:

Results and Discussions

4.1 Fabrication of Graphene Oxide (GO) Scroll

4.1.1 Introduction

Carbon nanoscroll (CNS) or in this dissertation is referred to as GO scroll and is studied due to its unique structure. GO scroll is similar to multi-wall carbon nanotube (CNT)[103-105] in which graphene sheets were rolled in certain angles to form cylindrical structure. However, CNT contains end-caps[106] while GO scroll had none. The non-existence of the end-caps enable extensive potential applications in the field of supercapacitors/batteries[53, 107], hydrogen storage[50, 52] and nanodevices[108-111]. GO scrolls as supercapacitors were theoretically calculated to have increased capacitance due to the availability of the exposed surface area.[53] While GO scrolls as hydrogen storage material were predicted to have improved performance of 3 wt% of ambient atmosphere as GO scroll's interlayer distance is tuned by addition of intercalant.[50] The broad ranges of promising applications of GO scroll were known to be attributed by its topologically open structure. However, the lack of feasible method to produce high quality and high density GO scroll hindered the realization of such applications.

Here, we introduced a technique to produce GO scroll through molecular combing of GO sheets on hydrophobic substrates. The first use of molecular combing technique was demonstrated in 1994 to extend and align DNA molecules on a silanized surface by receding air-water interface.[60] It is confirmed again by Kudo, *et al.* in 2007 in which protruding

ends of λ-DNA molecules played an important role to anchor itself onto hydrophobic substrates and thus allowing itself to be stretch during molecular combing process.[112] Therefore, by utilizing molecular combing technique, study on the alignment and formation of GO scroll on hydrophobic substrates is performed.

In this section, fabrication of well-aligned GO scrolls in high density on hydrophobic substrates such as aged gold-coated substrate, PDMS film, PLLA film, and OTS-SiO_2/Si substrate are shown. The formation of GO scroll is verified by characterization techniques, and the effect of GO solution and GO sheet's size toward its formation are also studied. Gas sensing device made of reduced GO scroll are developed to detect toxic gas such as NO_2.

4.1.2 Synthesis and Characterization of GO Scroll

GO sheets, which are obtained from modified Hummers' method as described in section 3.2, are first diluted in Milli-Q water to concentration of ~0.1 mg/mL. The morphology and size of typical produced GO sheets was shown in SEM image of Figure 4 - 1. GO sheets were observed in various size ranging from 10 to 100 μm.

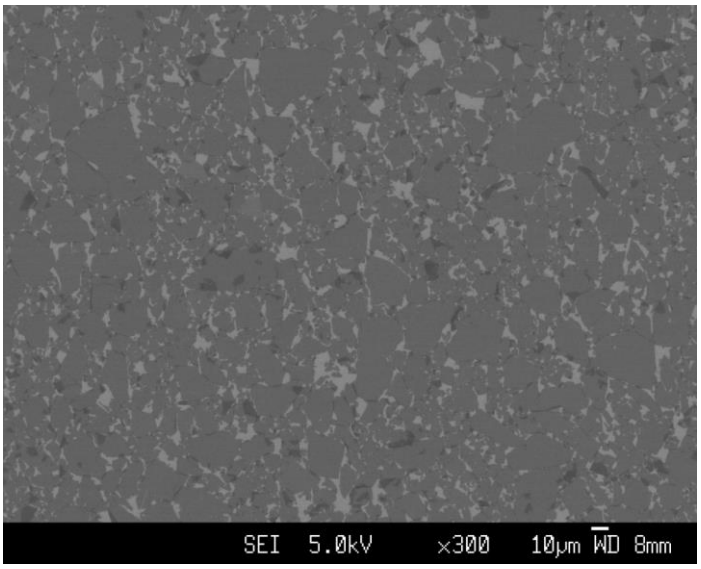

Figure 4 - 1. SEM image of GO sheets as synthesized by modified Hummers' method.[18] Reprinted with permission from John Wiley and Sons.

A schematic illustration in Figure 3 - 1 in section 3.3.2 describes the fabrication process of GO scrolls. Briefly, a clean glass coverslip is placed at angle of 45º to hydrophobic substrate on which there is solution of GO sheets. The glass coverslip is then pulled forward to the other end of substrate with hand. This movement created a control in direction of the alignment of GO scrolls as well as receding of water meniscus direction.

Substrates	Water Contact Angle (deg)
OTS-SiO_2/Si	**101.0 ± 2.6**
PLLA	**77.0 ± 0.8**
Gold-SiO_2/Si	**85.0 ± 0.4**
PDMS	**108.9 ± 1.9**

Table 1. Water contact angle measurement of various hydrophobic substrates (average value of n = 5).[18] Reprinted with permission from John Wiley and Sons.

Aged gold-coated SiO_2/Si as prepared in section 3.3.1.2 is used as hydrophobic substrate to demonstrate the fabrication of GO scrolls using molecular combing. Note that there is no washing step needed after molecular combing as all GO solution is swept off the substrate during combing. In this case, aged gold-coated SiO_2/Si is used instead of fresh gold-coated SiO_2/Si as fresh gold-coated SiO_2/Si was hydrophilic.[113-114] Hydrophillic fresh clean gold-coated SiO_2/Si turned into hydrophobic gold-coated SiO_2/Si as it is exposed to contamination from ambient environment overtime.[114] Therefore, aged gold-coated SiO_2/Si was used as hydrophobic substrate with measured water contact angle of 85^o as shown on Table 1.

The fabricated GO scrolls are then characterized by optical microscopy, AFM, Raman spectroscopy and TEM as shown in Figure 4 - 2. As depicted in Figure 4 - 2A and B, GO scrolls as seen from optical microscopy were aligned in a certain direction. The direction is governed by the direction of molecular combing process. GO scrolls produced are also shown in various lengths but also in high density. AFM is also used to characterize GO scrolls as seen on Figure 4 - 2C with height of measured scrolls larger than 10 nm (as

represented on Figure 4 - 2E). Raman mapping is performed on the same scrolls which shows high intensity of raman signal of GO (Figure 4 - 2D). Characteristic Raman spectrums of GO were observed in 1355 cm^{-1} and 1575 cm^{-1} as D band and G band respectively, [115-116] in which intensity increases as height of scrolls increases. (as observed in Figure 4 - 2F). Figure 4 - 2G revealed that the GO is loosely scrolled. The loose GO scroll is therefore has large interlayer distance which can be beneficial for potential application such as hydrogen storage or gas/molecule sensors.

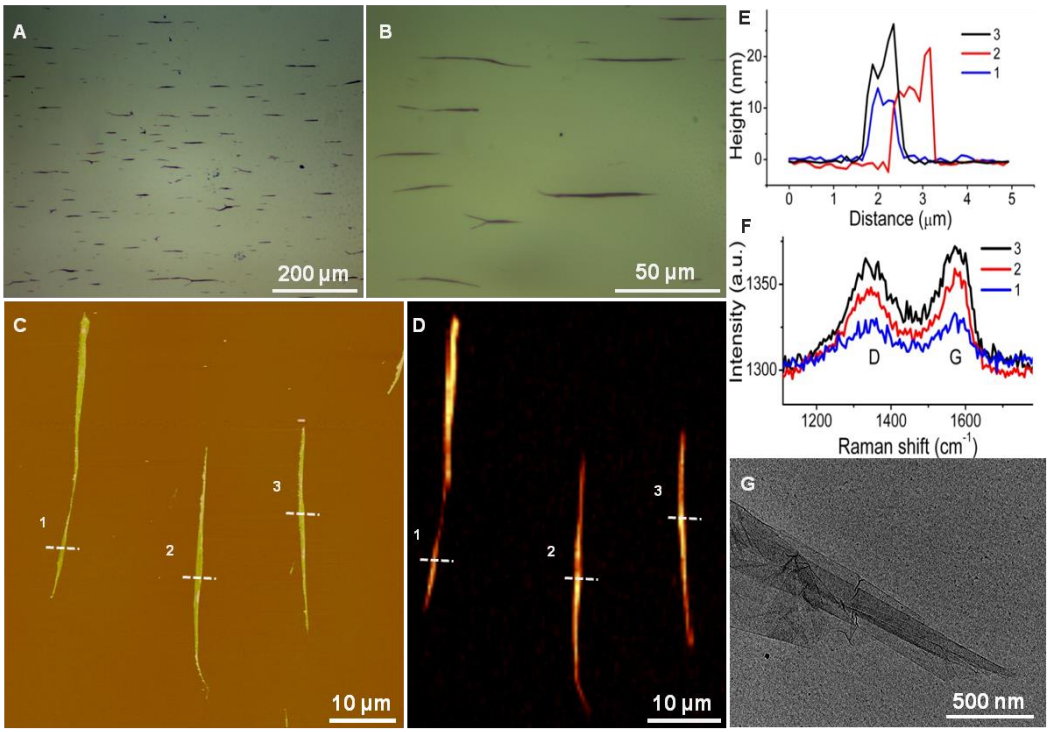

Figure 4 - 2. GO scrolls produced on an aged gold-coated SiO_2/Si by molecular combing. Optical images at (A) low magnification and (B) high magnification of GO scrolls. (C) Tapping mode AFM image of GO scrolls and (D) its respective Raman mapping. (E) GO scrolls height profiles as measured by AFM along the dotted lines marked in (C). (F) Raman spectra of GO scrolls on the dotted lines in (D). (G) TEM image of GO scroll.[18] Reprinted with permission from John Wiley and Sons.

Various other hydrophobic substrates are used in molecular combing process to demonstrate the versatility of this technique to produce GO scrolls. Hydrophobic substrates, such as OTS-SiO_2/Si, and spin-coated PLLA and PDMS film, are prepared as described in the section 3.3.1 and utilized as substrates for molecular combing. Their water contact angle are first determined, which are 101 ± 3°, 77 ± 1°, and 109 ± 2° for OTS-SiO_2/Si, PLLA and PDMS film, respectively (Table 1). Molecular combing of GO sheets in Milli-Q water on these substrates are performed and imaged by optical microscopy (Figure 4 - 3). GO scrolls are observed on all hydrophobic substrates which further validate the versatility of this technique. Note that the bubbles observed in Figure 4 - 3B were created during PLLA spin-coating process. Since these bubbles' surface is made of hydrophobic PLLA, no significant effect is observed on formation of GO scrolls.

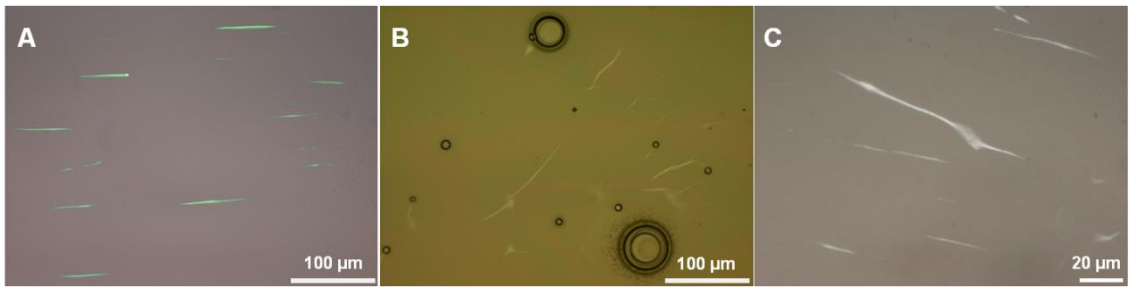

Figure 4 - 3. Optical images of the produced GO scrolls on different hydrophobic substrates of (A) OTS-SiO_2/Si (B) spin-coated PLLA film and (C) PDMS film.[18] Reprinted with permission from John Wiley and Sons.

4.1.3 Effects of Substrates and GO Solution

In order to study the mechanism of GO scrolls formation, the effect of substrates on the formation of GO scrolls by molecular combing are studied. In this case, hydrophilic SiO_2/Si is used as a substrate for molecular combing with GO solution in Milli-Q water. After molecular combing, no GO scroll is observed as seen in Figure 4 - 4. GO which are deposited on the hydrophilic substrates after molecular combing revealed sheets configuration instead of scroll. The findings are supported by molecular dynamics study performed in 2010 which concluded that folding of GO is possible if it is supported on hydrophobic substrate but not on hydrophilic substrate.[117] The attraction of graphene and hydrophilic substrate is too strong which prevented graphene sheets from folding. However, the weaker attraction between graphene and hydrophobic substrate allowed graphene to fold due to molecular interactions with water.

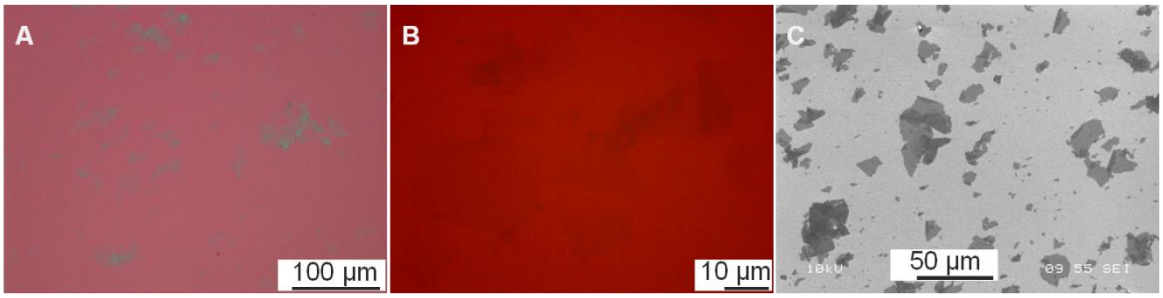

Figure 4 - 4. (A) Low, (B) high magnification optical images and (C) SEM image of GO sheets after molecular combing on hydrophilic SiO_2/Si substrate.[18] Reprinted with permission from John Wiley and Sons.

Another variable to be considered in the formation of GO scroll mechanism is the solvent in which GO sheets were dissolved in. Ethanol is introduced into GO in water solution in various volume ratio of ethanol : water = 9 : 1 (Figure 4 - 5A,B), ethanol : water

= 1 : 1 (Figure 4 - 5C,D), and ethanol : water = 1 : 9 (Figure 4 - 5E,F). Molecular combing is performed with GO sheets dissolved in mixture of ethanol and water solution on hydrophobic substrates and immediately imaged as shown in Figure 4 - 5. There is no GO scroll observed on the Figure 4 - 5A,B as 90% of GO solution contained ethanol. As the percentage of ethanol is decreased into 50% in the solution, GO sheets were observed to be loosely folded (Figure 4 - 5C,D). In addition, as the ethanol amount was further reduced to 10%, GO scroll formation after molecular combing is observed (Figure 4 - 5E,F).

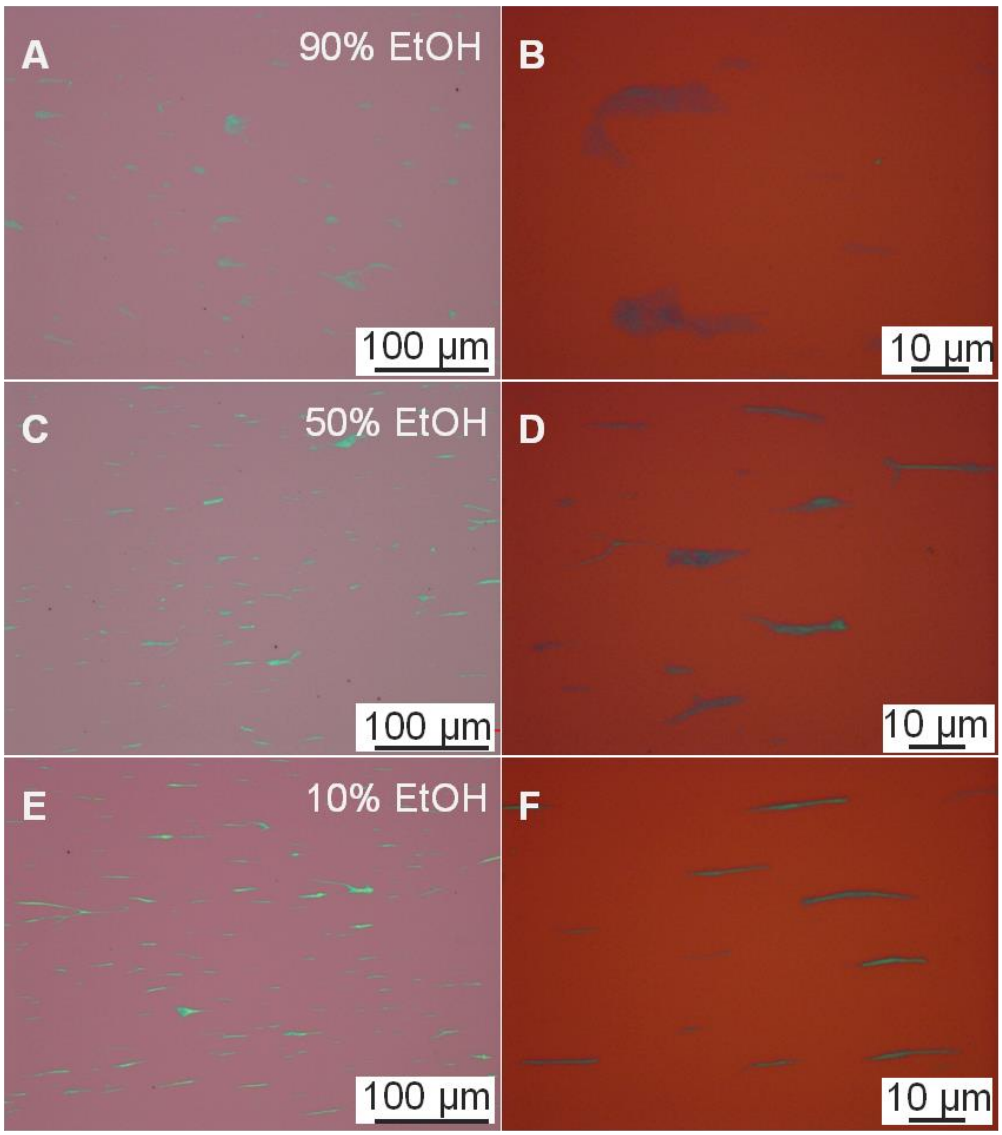

Figure 4 - 5. Optical images of folded/scrolled GO structures on OTS-SiO_2/Si which is fabricated by molecular combing of GO sheets in solution with different volume ratio of ethanol to water. (A-B) GO in 90% ethanol : 10% water solution. (C-D) GO in 50% ethanol : 50% water solution. (E-F) GO in 10% ethanol : 90% water solution.[18] Reprinted with permission from John Wiley and Sons.

The critical role played by water in the formation of GO scroll is proven in the experiment above. It is regarded as one of the driving force towards the folding and then scrolling of GO sheets. Previously, capillary interaction is reported to clarify polymers or Si sheets folding mechanism of on hydrophobic substrates which are mediated by water droplet.[118-119] In these reports, the capillary force at the junction of receding water meniscus - 2D material - air was the main driving force to cause the extremities of 2D material sheet to spontaneously pull up and thus fold or scroll. It is also widely reported that during molecular combing process, DNA molecules are linearly attached onto hydrophobic substrates due to interactions between hydrophobic DNA nucleobases chain and the substrates.[60, 112, 120-121] Similarly, in this dissertation, there are two actions which led to the formation of well aligned GO scrolls, namely, hydrophobic interaction between GO sheets and hydrophobic substrate and dewetting of GO sheets in Milli-Q water solution from hydrophobic substrate. Firstly, hydrophobic interaction between GO sheets and hydrophobic substrates contributed to the pinning of GO sheets on hydrophobic substrates via hydrophobic interactions. Secondly, the dewetting of GO sheets in Milli-Q water solution allowed the capillary force to induce the folding or scrolling of GO sheets spontaneously on hydrophobic substrates and stretched GO sheets in the direction of receding water meniscus.

4.1.4 Gas Sensing Application

In order to demonstrate the potential application of GO scroll, a proof of concept gas sensing device was fabricated with single rGO scroll as channel material (Figure 4 - 6). GO scrolls which are fabricated on OTS-SiO_2/Si are first reduced by hydrazine vapor [99] to

obtain rGO scrolls followed by deposition of gold as source and drain electrodes as described in section 3.6.6. The optical image of resulting device is depicted in Figure 4 - 6 inset. A single rGO scroll exhibited linear characteristics of current - voltage curve measured in the range of - 2 to 2 V as shown in Figure 4 - 6A.

Resistance of rGO scroll is measured as ~2.5×10^7 Ω in Figure 4 - 6 A. Its resistivity (ρ) can be calculated by using the following equation[54]

$$\boldsymbol{\rho} = \boldsymbol{R}\frac{\boldsymbol{A}}{\boldsymbol{l}}, \quad (1)$$

where R = resistance (Ω), A = cross sectional area of channel material (m^2), and l = length of channel material (m). Average height and width of rGO scroll of ~20 and 600 nm were used in cross section area calculation which resulted in ~1.2×10^{-14} m^2. The resistivity of this rGO scroll is projected to be ~1×10^{-2} Ω·m taking l as ~3×10^{-5} m (Figure 4 - 6 inset). This resistivity value however is much larger than graphene scrolls made of mechanically exfoliated graphene sheet which is ~ 2.8×10^{-6} Ω·m.[47]

The produced single rGO scroll device is then used as gas sensor to detect low concentration of NO_2 gas at room temperature. NO_2 gas with concentration ranging from 0.4 to 2 ppm was injected into glove box in which rGO scroll device was probed. Figure 4 - 6C showed the current response upon exposure of NO_2 gas. An obvious increase in current was observed upon first exposure to NO_2 gas concentration of 0.4 ppm. The trend of current increase is attributed to the *p*-doping effect,[13-15] which was also observed in graphene[122] and carbon nanotube[123] based sensor devices. NO_2 which is a strong oxidizer can withdraw electron from *p*-type rGO scroll and transfer it to adsorbed NO_2 molecules. Electron withdrawal caused increase in hole concentration in rGO scroll and subsequently increase its' conductivity.[122] The slow response time is owed to the room temperature sensing

experiment which is also reported previously in rGO based film NO_2 gas sensor.[124-125] Detection limit of rGO scroll based NO_2 gas sensor is calculated as followed,

$$\boldsymbol{DL = 3 \times \frac{C_{NO_2}}{\frac{S}{N}}}, \qquad (2)$$

where DL = detection limit (ppm), C_{NO2} = concentration of NO_2 gas (ppm), S = current at saturation - current at background and N = standard deviation of background current. Detection limit of this rGO scroll based NO_2 gas sensor is therefore estimated to be 56 ppb based on signal to noise ratio of 3.

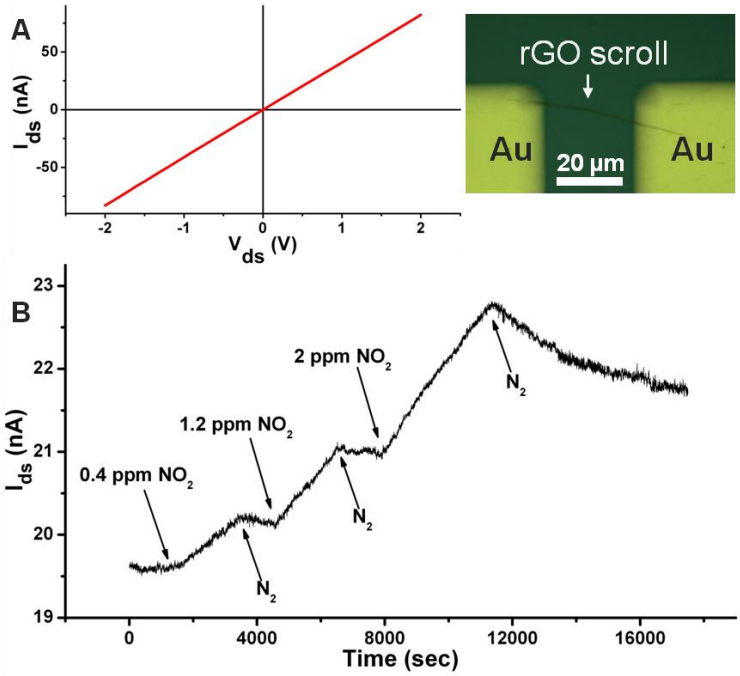

Figure 4 - 6. Gas sensor device made of a single rGO scroll as channel material. (A) I_d - V_d characteristic curve measured on a single rGO scroll device. (B) Real-time current response as single rGO scroll device is exposed to NO_2 gas with varying concentration. Inset: Optical image of the produced single rGO scroll device. [18] Reprinted with permission from John Wiley and Sons.

4.1.5 Short Summary

In conclusion, a simple and efficient technique is developed to produce high density and well-aligned GO scrolls on hydrophobic substrates. Various hydrophobic substrates including aged gold-coated SiO_2/Si, OTS-SiO_2/Si, spin-coated PLLA and PDMS films are used to demonstrate the versatility of this technique. Characterization of the fabricated GO scrolls showed GO scrolls were loosely scrolled and in diverse length and width. Substrates hydrophobicity as well as GO sheets solvent is proven to be crucial in the formation of GO scroll. A single rGO scroll is successfully used as a channel material in NO_2 gas sensor device with detection limit of 56 ppb.

4.2 Fabrication of Other Graphene Oxide (GO) Architectures

4.2.1 Introduction

In the previous section, it has been shown that GO scrolls can be fabricated only on hydrophobic substrates via molecular combing technique.[18] It is therefore intriguing to explore the effect of coexisting hydrophilic-hydrophobic region on substrates towards the creation of GO architectures. The coexisting hydrophilic-hydrophobic region has been widely fabricated and studied through patterning of self-assembled monolayers (SAMs) due to numerous available surface functionalities and its ease of fabrication.[77] It has also been reported previously that assembly of new structures can be formed on substrates with hydrophilic-hydrophobic micro- and nano-patterned SAMs such as polymer rings,[78] carbon nanotube rings, carbon nanotube line arrays and filtration membranes.[81] The most efficient and versatile technique in fabricating hydrophilic-hydrophobic patterned surfaces

over a large area is micro-contact printing (μCP).[126-127] Subsequently, micro-contact printing is performed to produce hydrophilic-hydrophobic patterned substrate.

In this section, fabrication of GO architectures resulted from molecular combing of GO sheets on hydrophilic-hydrophobic micro-patterned SAMs are reported. A novel GO architecture is shown on dotted hydrophilic SAMs pattern which is labelled as beaded GO string. The shape, orientation and position of GO sheets can be potentially controlled by hydrophilic-hydrophobic micro-patterned SAMs on substrate. The effect of variables such as molecular combing speed, GO sheets concentration in water, and GO sheets size in the formation of beaded GO string are also studied. The effect of surface functionalities is also explored in order to determine the mechanism of GO architecture formation. In addition, a gas sensing device with a single beaded rGO string as channel material is also fabricated to investigate its gas sensing performance.

4.2.2 Synthesis and Characterization of Other GO Architectures

GO sheets are produced by modified Hummers' method as described in section 3.2. The used solution of GO sheets is further diluted to ~0.1 mg/mL unless otherwise stated. In the section 3.4.1 and 3.4.2, the formation of hydrophilic-hydrophobic patterned region is described in details followed by the molecular combing process of the aqueous solution of GO sheets. In short, the hydrophilic-hydrophobic SAMs region is patterned with PDMS stamp which contained dot or line features on Au substrates. Molecular combing of GO sheets is then performed on hydrophilic-hydrophobic micro-patterned substrates as illustrated by Figure 3 - 2.

Dotted MHA-ODT pattern substrates are first used to demonstrate the formation of unique GO architecture as seen in Figure 4 - 7. Optical images in Figure 4 - 7A and B indicate the formation of GO architecture named beaded GO string on 5 μm - 5 μm and 10 μm - 10 μm dotted MHA-ODT pattern respectively. It is observed that a single beaded GO string consist of alternating bead-like and string-like structures. Further characterization of beaded GO string is performed by SEM as observed in Figure 4 - 7C. Darker dotted region observed in the SEM image corresponds to MHA patterned area while brighter region corresponds to ODT patterned area. The SEM image reveals that the bead-like portion of beaded GO string is always exist on the dotted MHA pattern area while the string-like portion of beaded GO string is always lie on the passivated ODT region. In addition, AFM image in Figure 4 - 7D observes the morphology of beaded GO string. In which a slightly folded GO sheets is seen as bead-like region whereas a densely folded GO sheets is seen as string-like region. Its' height profiles showed that the bead-like GO sheets portion has a maximum height of ~23.4 nm which is approximately one-third of the height profiles of string-like portion of ~64.6 nm. This observation is also supported and shown in TEM image of beaded GO string (Figure 4 - 7G). In addition, beaded GO string maintained its structure even after transfer on holey carbon TEM grid which implies high stability. Raman spectroscopy is also performed as shown in Figure 4 - 7E, F. Similar to GO scrolls, characteristics Raman spectra for graphene oxide are observed by the existence of D and G band of 1355cm^{-1} and 1600 cm^{-1}. Raman mapping of GO architecture in the range of 1000 - 1800 cm^{-1} is performed and indicates higher Raman signal intensity on the string-like (ODT) region in comparison to bead-like (MHA) region. This behavior is similar to

previous section in which Raman intensity signal increases as height of GO scroll produced increases.

Molecular combing is also performed on different MHA dot feature size. The beaded GO string architectures are shown to be successfully fabricated with dotted MHA pattern ranging from 2 μm - 2 μm (Figure 4 - 9A), 5 μm - 5 μm (Figure 4 - 7A), 10 μm - 10 μm (Figure 4 - 7B, 4 - 9B), and 20 μm - 20 μm (Figure 4 - 9C) features. Therefore, the versatility of this beaded GO string architecture formation is demonstrated.

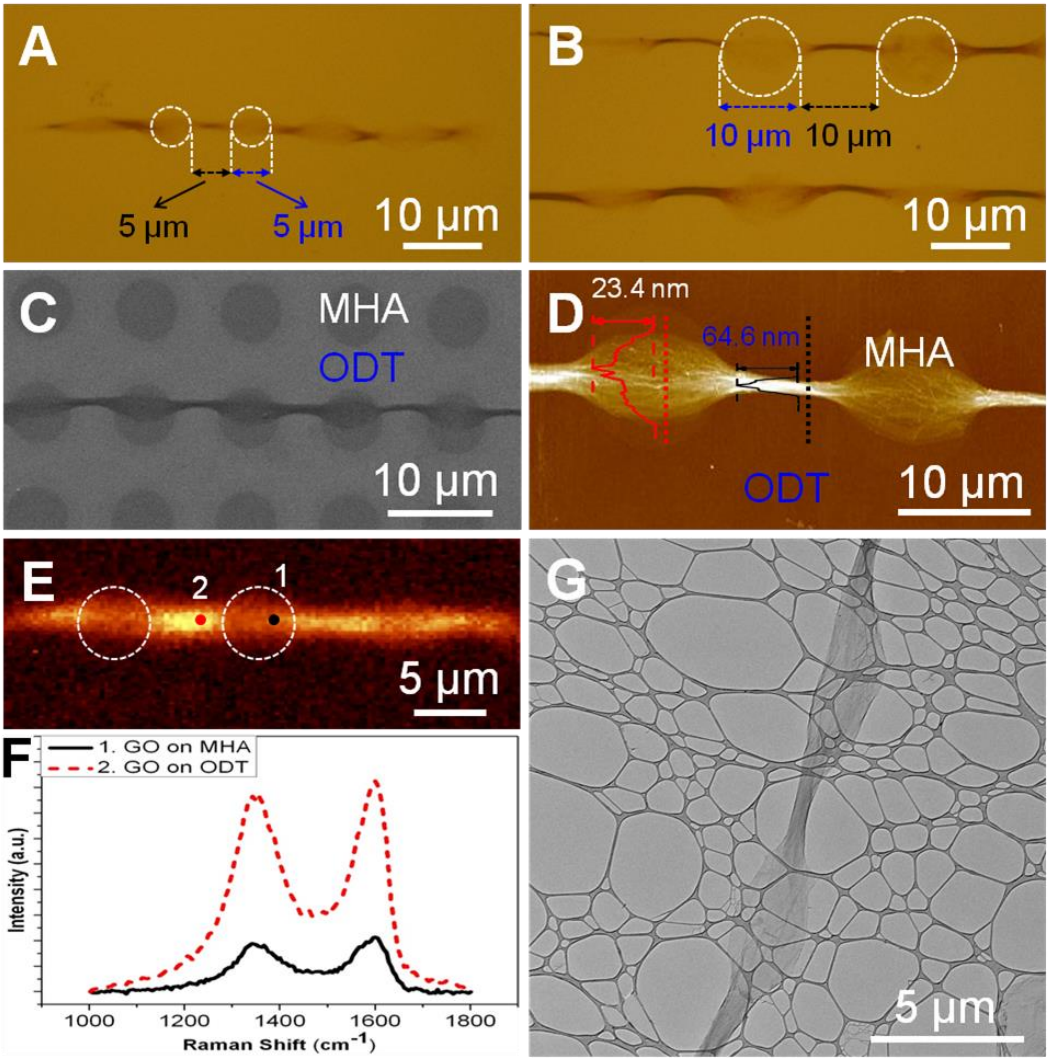

Figure 4 - 7. Characterization of the fabricated novel GO architectures. Optical images of GO architecture fabricated on (A) 5 µm - 5 µm (B) 10 µm - 10 µm dotted feature of MHA-ODT patterns. (C) SEM, (E) Raman mapping and (G) TEM image of GO architecture fabricated on 5 µm - 5 µm dotted feature of MHA-ODT patterns. (D) AFM image of GO architecture fabricated on 10 µm - 10 µm dotted feature of MHA-ODT patterns. (F) Raman spectra of GO architecture at areas specified by the black dot (1) and red dot (2) in (E). The dotted circled in (A), (B) and (E) designate the region of dotted MHA patterns.[102] Reprinted with permission from John Wiley and Sons.

PDMS stamps with feature consisting of same sized line and gap, are also used to create lined MHA patterns on gold-coated SiO_2/Si. After ODT passivation, molecular combing of GO sheets in water is executed in the direction parallel to the lined MHA patterns as shown in Figure 3 - 2C,D. Figure 4 - 8A, B illustrate the optical and SEM images of the resulting GO architectures after molecular combing on 2 μm - 2 μm lined feature of MHA patterns. GO sheets are found to be folded and preferably aligned itself on the hydrophilic region of lined MHA pattern rather than on hydrophobic ODT region. This phenomenon is also observed on lined MHA patterns with 5, 10 and 20 μm feature sizes (Figure 4 - 9D-F). μCP technique has been used to create these lined MHA patterns easily and can be subsequently used as templates to confine and direct the arrangement of GO sheets.

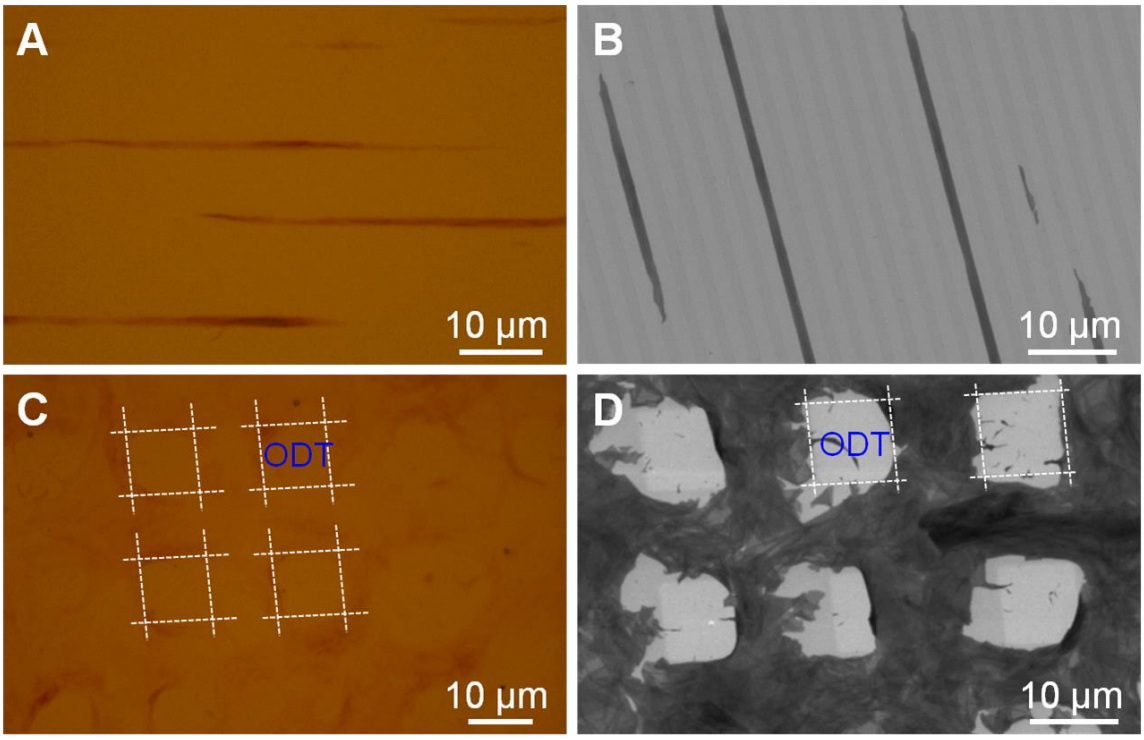

Figure 4 - 8. (A) Optical image and (B) SEM image of GO sheets confined in stripe shape fabricated on 2 μm - 2 μm lined feature of MHA-ODT patterns. (C) Optical image and (D) SEM image of GO sheets confined in cross feature fabricated on 10 μm - 10 μm crossed feature of MHA-ODT patterns. The area surrounded by the dotted lines in (C) and (D) are designated as ODT-passivated region.[102] Reprinted with permission from John Wiley and Sons.

Another example in which crossed MHA patterns are fabricated by using μCP. PDMS stamp with 10 μm line feature is inked with MHA molecules and printed on gold-coated substrate twice which are in horizontal and vertical directions. Apparently, after molecular combing, GO sheets are found to settle on MHA SAMs region compared to ODT SAMs region, as depicted in Figure 4 - 8C, D. As GO sheets preferably resided on MHA SAMs region, GO sheets are folded and stacked on each other to avoid or minimize contact

with ODT SAMs region. Therefore, continuous GO sheets in cross pattern with pore size of 10 µm can be observed. The pore size which corresponds to the PDMS line feature size can therefore be easily manipulated hence unlock a potential technique to produce GO network with controllable pore size.

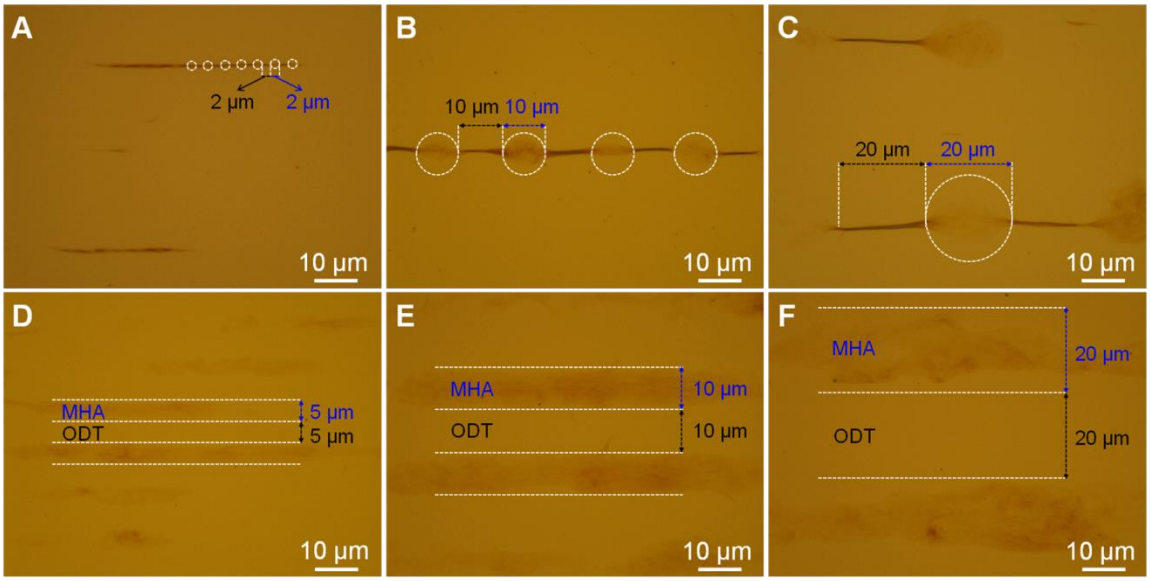

Figure 4 - 9. Optical images of patterned GO architecture on various sized and feature of MHA-ODT patterns. GO architectures produced on (A) 2 µm - 2 µm, (B) 10 µm - 10 µm and (C) 20 µm - 20 µm dotted MHA-ODT patterns. Lined GO architectures produced on (D) 5 µm - 5 µm, (E) 10 µm - 10 µm and (F) 20 µm - 20 µm lined MHA-ODT patterns. The area surrounded by the dotted circles indicated dotted MHA pattern region.[102] Reprinted with permission from John Wiley and Sons.

4.2.3 Effects of Molecular Combing Variables in GO Architectures Formation

Systematic study is performed to demonstrate the effect of molecular combing variables such as molecular combing speed, size and concentration of GO sheets in water solution on the formation of GO architecture. Previously in Figure 4 - 9, it has been proven

that the size of MHA patterns feature did not have influence on the formation of GO architecture both on dotted and lined MHA pattern. In this sub-section, 10 µm - 10 µm dotted MHA pattern will be used to study the effect of other molecular combing variables.

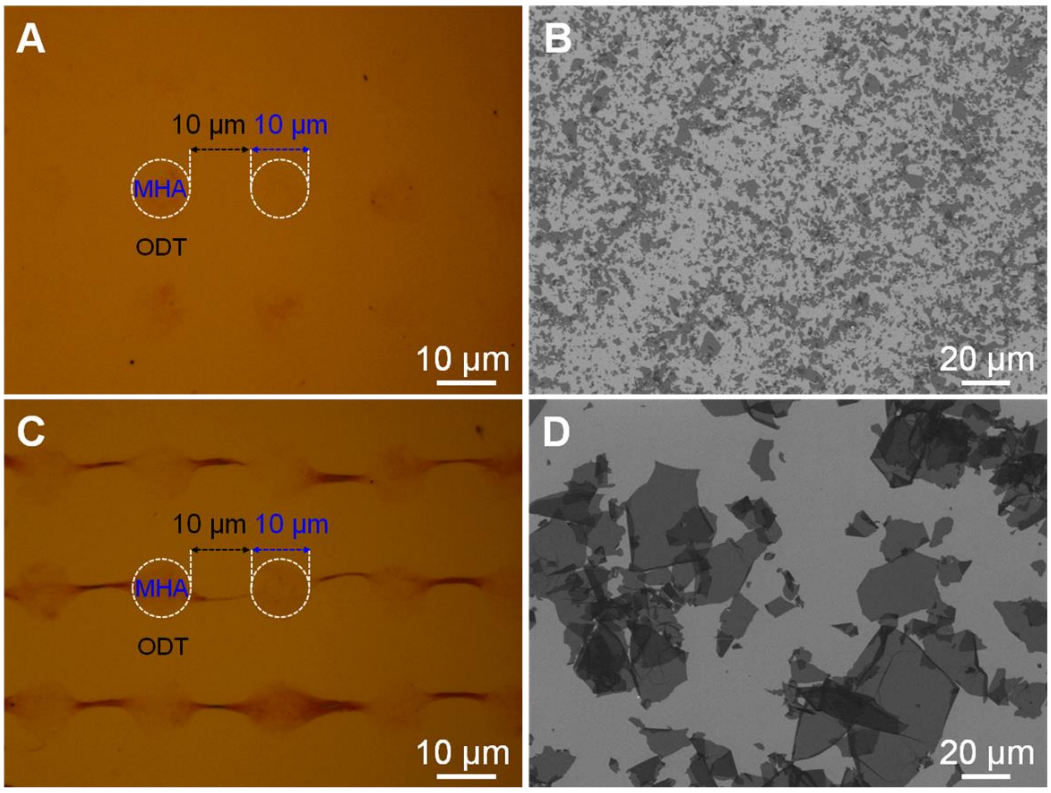

Figure 4 - 10. (A, C) Optical images of GO architectures produced by molecular combing of 0.8 mg/mL GO sheets solution in water on 10 µm - 10 µm dotted feature of MHA-ODT patterns with 3 mm/s speed. (A, B) small-sized GO (< 10 µm) and (C, D) large-sized GO sheets (> 20 µm) which are utilized for molecular combing. (B, D) SEM images of the corresponding GO sheets used for molecular combing in (A) and (C) respectively. Dotted circles in (A) and (C) corresponds to the MHA patterned area.[102] Reprinted with permission from John Wiley and Sons.

By varying the GO sheets size used for molecular combing, GO sheets size was categorized into two, small-sized GO sheets which are smaller than 10 μm (Figure 4 - 10B) and large-sized GO sheets which are larger than 20 μm (Figure 4 - 10D). Small sized GO sheets are obtained from sonication of large-sized GO sheets as produced by modified Hummers' method for 30 min. As seen from optical image in Figure 4 - 10A, no beaded GO string architecture was observed when small-sized GO sheets are used in molecular combing. SEM image in Figure 4 - 11 further verified this observation. Small-sized GO sheets are preferably spread and reside within patterned MHA SAMs area. This observation is also confirmed in lined and crossed MHA pattern in which large-sized GO sheets favored MHA pattern region. In the other hand, when large-sized GO sheets of the same concentration are used during molecular combing on dotted MHA pattern, beaded GO string can be fabricated (Figure 4 - 10C).

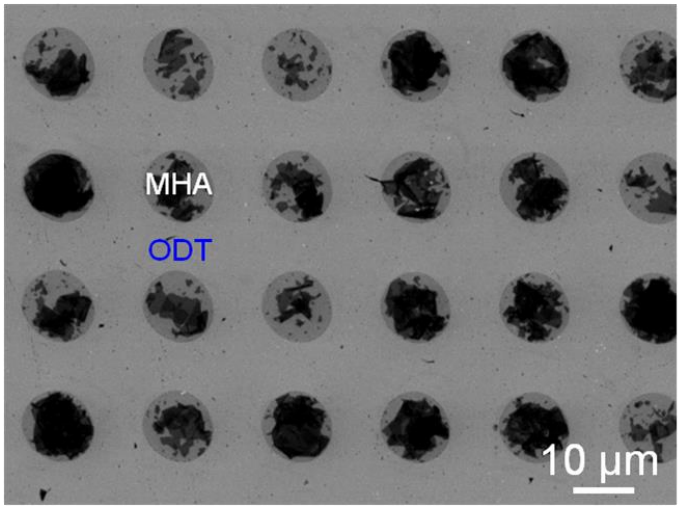

Figure 4 - 11. SEM image of GO architectures produced by molecular combing speed of 3 mm/s with 0.8 mg/mL small sized GO (< 10 μm) in water solution. The molecular combing process is performed on 10 μm - 10 μm dotted feature of MHA-ODT patterns.[102] Reprinted with permission from John Wiley and Sons.

Apart from GO sheets size, the effect of GO sheets concentration in water on GO architecture formation was also investigated. As shown in Figure 4 - 12, molecular combing of large-sized GO sheets is executed on 10 μm - 10 μm dotted feature of MHA pattern with speed of 3 mm/s. GO sheets concentration is varied from 0.2 mg/mL (Figure 4 - 12A), 0.4 mg/mL (Figure 4 - 12B) and 0.8 mg/mL (Figure 4 - 12C). Beaded GO string architectures are observed in all occasions but in different coverage percentage. The coverage percentage of dotted MHA pattern by the resulting beaded GO string is increased as the GO sheets concentration in water increases. In this case, coverage percentage (*C*) is determined as ratio of the quantity of beaded GO strings unit to the quantity of MHA dots observed in 20 × optical image, as described in Equation 3 below. One beaded GO string unit is defined to consist of 1 GO bead on MHA region and 1 neighboring GO string on ODT region as illustrated in inset of Figure 4 - 12D.

$$\boldsymbol{C = \frac{N_{GO}}{N_{MHA}} \times 100\%} \qquad (3)$$

where, C = percentage of dotted MHA pattern covered by the resulting beaded GO strings, N_{GO} = amount of beaded GO string units in 20 × optical image objective, and N_{MHA} = number of MHA dots in 20 × optical image objective.

Based on optical images taken after molecular combing with GO sheets concentration in water of approximately 0.2 mg/mL, 0.4 mg/mL and 0.8 mg/mL; coverage percentage is calculated to be 18 ± 4%, 41 ± 8% and 84 ± 2% respectively (Figure 4 - 12D). The formation of beaded GO string is observed to be linearly correlated to the concentration of GO sheets in water used during molecular combing.

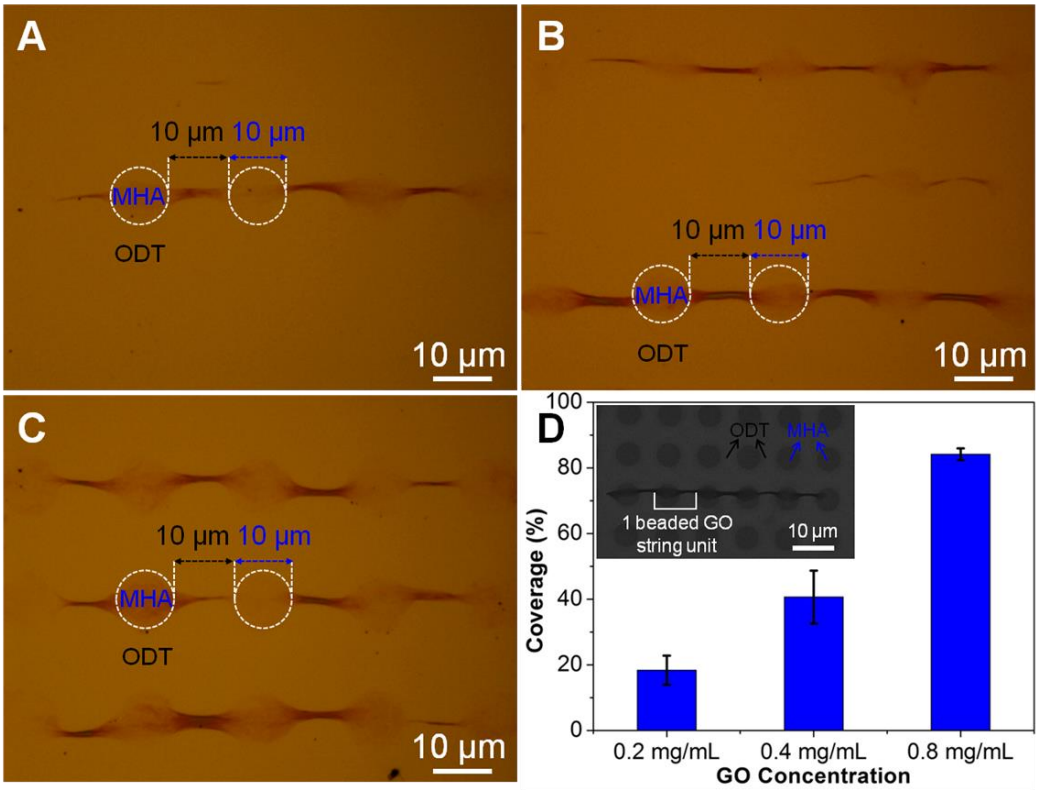

Figure 4 - 12. Fabrication of GO architectures by molecular combing of large-sized GO sheets (larger than 20 μm) at various concentrations with a speed of 3 mm/s on 10 μm - 10 μm dotted feature of MHA-ODT patterns. Optical image of the resulting GO architectures with (A) 0.2 mg/mL, (B) 0.4 mg/mL and (C) 0.8 mg/mL concentration of GO in water. (D) Coverage percentage of the resulting beaded GO string at various GO concentration. Inset: SEM image of beaded GO string on 5 μm - 5 μm dotted feature of MHA-ODT patterns.[102] Reprinted with permission from John Wiley and Sons.

In the other hand, Figure 4 - 13 shows beaded GO string fabricated by molecular combing of large-sized GO sheets at 0.2 mg/mL concentration on 10 μm - 10 μm dotted feature of MHA patterns with varying speed. Optical images of beaded GO string produced at molecular combing speed of 1 mm/s (Figure 4 - 13A), 3 mm/s (Figure 4 - 13B) and 10

mm/s (Figure 4 - 13C) does not show any morphological anomaly. However, as molecular combing speed is increased from 1 mm/s to 3 mm/s to 10 mm/s, the coverage percentage is reduced to 37 ± 5%, 18 ± 4% and 8 ± 3% respectively (Figure 4 - 13D). This observation is due to the insufficient time for GO sheets to attach themselves on hydrophobic substrates as the molecular combing speed increases, which resulted in lower coverage percentage.

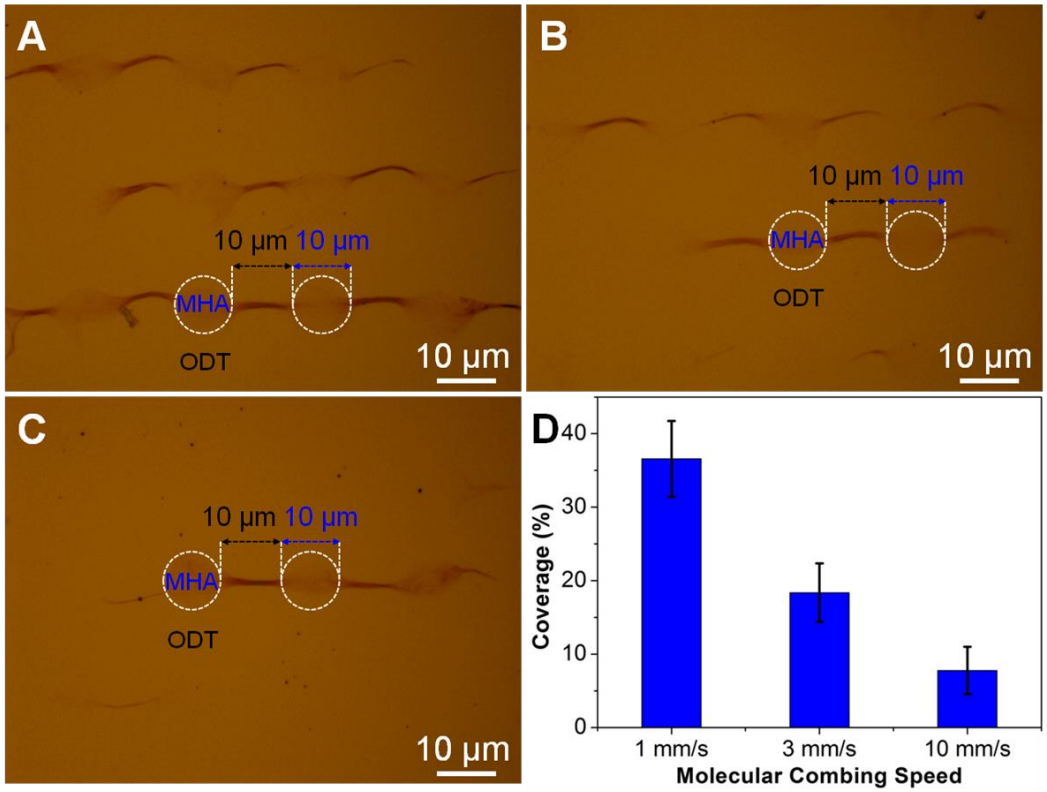

Figure 4 - 13. Fabrication of GO architectures via molecular combing of large-sized GO sheets (larger than 20 µm) with 0.2 mg/mL concentration on 10 µm - 10 µm dotted feature of MHA-ODT patterns at various speed. Optical images of the resulting GO architectures with (A) 1 mm/s, (B) 3 mm/s and (C) 10 mm/s molecular combing speed. (D) Coverage percentage of the resulting beaded GO string at various molecular combing speed.[102] Reprinted with permission from John Wiley and Sons.

GO sheets showed better wetting property or preference to MHA SAMs region compared to ODT SAMs region in all experimental results described above. This observation might be contributed by the interaction between GO sheets and MHA or ODT SAMs. Hydrophilicity and hydrophobicity of the substrate surface are resulted from the existence of these SAMs which modify the interaction between water and the substrate surface. Hydrophobic substrate is fabricated when the cohesive force of bulk water is lower than the interaction force between water and the surface.[128] Water contact angle measurements are then performed on GO film, MHA and ODT SAMs to determine its surface wettability as shown in Figure 4 - 14. Single layer GO film on SiO_2/Si was obtained by Langmuir-Blodgett film deposition technique, while MHA and ODT SAMs covered gold-coated SiO_2/Si were obtained by immersing gold-coated SiO_2/Si into MHA or ODT solution for 30 min. GO film water contact angle is measured as 37.8 ± 1.7^o,[129] while MHA and ODT SAMs had water contact angle of 17.8 ± 4.5^o and 96.2 ± 2.7^o respectively. Water contact angle measurement further confirmed the formation of alternative region of hydrophilic MHA and hydrophobic ODT SAMs on gold-coated SiO_2/Si. Therefore, during molecular combing process, as hydrophilic GO sheets encounter and interact with hydrophilic MHA SAMs region, folding of GO sheets are not encouraged. In contrary, as hydrophilic GO sheets encounter hydrophobic ODT SAMs region, minimum interaction occurred and therefore folding of GO sheets took place. This mechanism is also consistent with work presented in the previous section which GO sheets fold or scroll on hydrophobic substrate but spread on hydrophilic substrate.[18] Consequently, a unique GO architecture in the form of beaded GO string was fabricated.

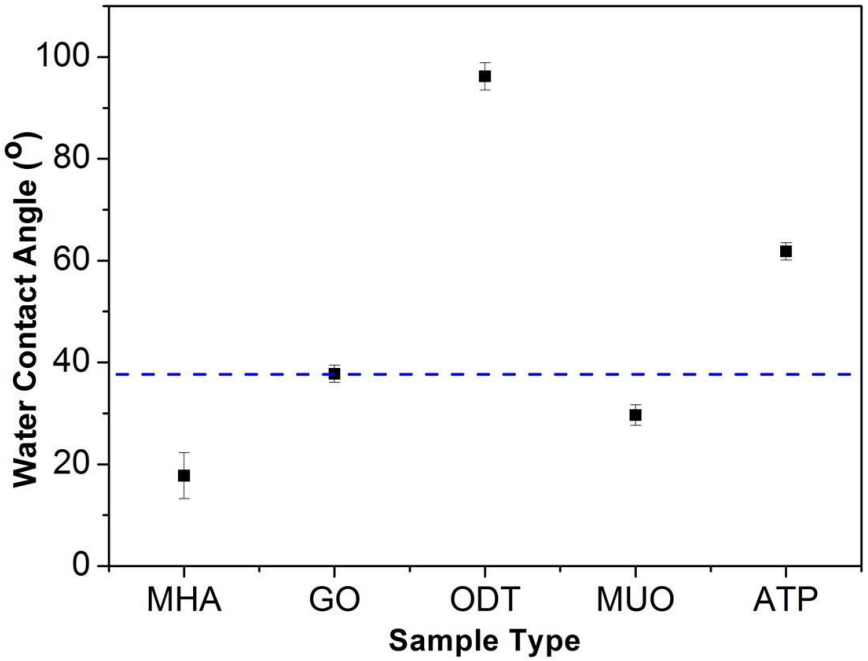

Figure 4 - 14. Water contact angles measurement of GO film, MHA, ODT, MUO, and ATP SAMs on gold-coated SiO_2/Si.[102] Reprinted with permission from John Wiley and Sons.

To further substantiate the mechanism proposed, SAMs with different functional groups are used instead of MHA. MHA with -COOH functional group is replaced with 11-mercapto-1-undecanol (MUO) which has -OH group or 4-aminothiophenol (ATP) which has -NH_2 functional group. Water contact angle of MUO and ATP SAMs on gold-coated SiO_2/Si are first measured as shown in Figure 4 - 14 which are 29.7 ± 2.0° and 61.8 ± 1.7° respectively. MUO and ATP are used as inking molecules during μCP with 5 μm dot feature PDMS stamp to form dot arrays on gold-coated SiO_2/Si. ODT is also used as blocking layer on the non-inked region as described in experimental details section 3.4.1.2. Molecular combing of GO sheets is performed on MUO-ODT and ATP-ODT SAMs patterned substrate and characterized with optical microscopy and SEM as shown in Figure 4 - 15.

Optical image in Figure 4 - 15A observes the formation of beaded GO string on dotted MUO pattern while no noticeable beaded GO string is seen on dotted feature of ATP pattern in Figure 4 - 15C. The result is supported by SEM images in Figure 4 - 15B, D, in which successful printing of both dotted MUO and ATP SAMs can be visualized but absence of beaded GO string architectures is noticed only dotted ATP pattern. GO architecture observed on dotted ATP pattern resembled loosely folded GO sheets. This observation is attributed to water contact angle of ATP SAMs (61.8 ± 1.7^{o}) which is higher or more hydrophobic compared to GO sheets. Therefore, it can be concluded that surface interaction between GO sheets and hydrophilic-hydrophobic SAMs coated substrates is paramount driving force to the formation of novel GO architecture.

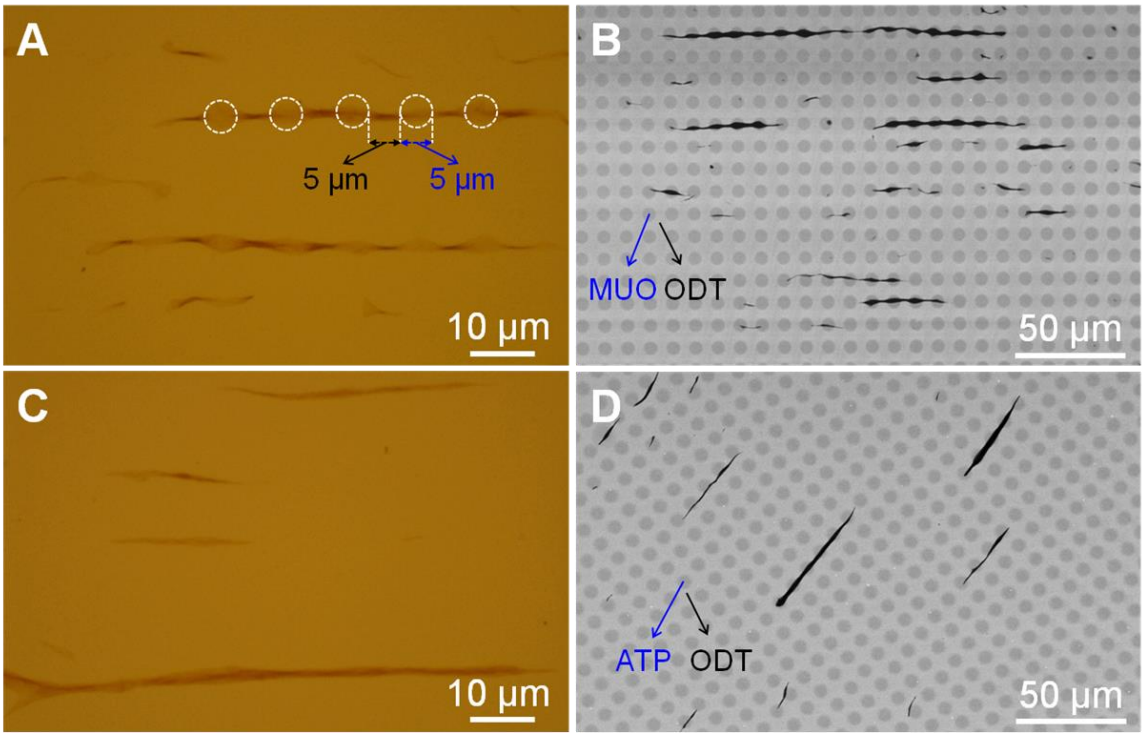

Figure 4 - 15. Optical images of GO architectures produced by molecular combing on dotted (A) MUO-ODT and (C) ATP-ODT patterns. SEM images of GO architectures produced by molecular combing on dotted (B) MUO-ODT and (D) ATP-ODT patterns. The areas surrounded by the dotted circles in (A) denote the dotted MUO patterns.[102] Reprinted with permission from John Wiley and Sons.

4.2.4 Gas Sensing Application

The fabricated beaded GO strings on gold-coated SiO_2/Si are firstly transferred on 300 nm SiO_2/Si before being reduced by hydrazine vapor. In brief, PLLA film is spin-coated on substrate containing beaded GO string, peeled off with PDMS film as support film and then transferred on 300 nm SiO_2/Si before dissolving off PLLA in DCM at 50^{o}C.[98] After reduction with hydrazine vapor, gold electrodes are then deposited on a single beaded rGO string to form source and drain electrodes (Figure 4 - 16A). Beaded GO string architecture

has shown stability during the transfer and reduction process with no morphological deformation observed. The fabricated device is made of a single beaded rGO string as channel material and utilized as NO_2 gas sensing device. Figure 4 - 16B,C displayed the NO_2 gas sensing performance of a beaded rGO string device at concentration of 0.5 ppm to 5.8 ppm. The positive change in current upon exposure of NO_2 gas is attributed to the *p*-doping effect[13-15] as observed for GO scroll based gas sensing device. The room temperature gas sensing device has calculated detection limit of 5.8 ppb based on signal to noise ratio of 3 (Equation 1). This detection limit is sufficient for practical NO_2 gas sensor which has an average 24-hour limit of NO_2 in air of 53 ppb.[130] In comparison to the fabricated single rGO scroll based gas sensor device, detection limit of single beaded rGO string is approximately one order magnitude higher. This better gas sensing performance is due to the increase surface area in beaded rGO string available for NO_2 gas absorption.

However, the produced GO scrolls as well as beaded GO strings used as NO_2 gas sensors do not outperform compared to previously reported GO sheets. GO sheets which were reduced by low temperature annealing have shown ability to detect 2 ppm NO_2 with current change of 12%.[124] Even though the observed current change is higher than the beaded rGO string based device, the observed noise level is also higher compared to the beaded rGO string. In another report of NO_2 gas sensor, GO sheets which reduced with vitamin C have shown detection limit of 400 ppt.[41] Compared to the rGO scroll and beaded rGO string, this detection limit is one/two order of magnitude higher. It might be due to the existence of large surface area.

On the other hand, the rGO scroll and beaded rGO string are comparable or better gas sensing materials compared to the semiconducting CNTs. NO_2 gas sensing mechanism

on CNTs is described to be similar to rGO sheets in which the adsorbed NO_2 gas molecule accepts electron from CNT/rGO sheets.[131,132] Single-walled CNTs (SWCNTs) on an interdigitated electrode have been reported as NO_2 gas sensor with detection limit of 44 ppb at room temperature.[133] Meanwhile, MWCNTs prepared by plasma enhanced chemical vapor deposition have also been reported to exhibit sensitivity towards NO_2 gas with detection limit of 10 ppb at operating temperature of 165 ^oC.[134] In addition, graphene in a three-dimensional porous architecture, referred as graphene foam, has been used as NO_2 gas sensing material. Graphene foam shows sensitivity of ~4% when exposed to 20 ppm NO_2 at room temperature. In comparison to the beaded rGO string which has sensitivity of >4% at 0.5 ppm NO_2, the performance graphene foam used as NO_2 gas sensing material is low.

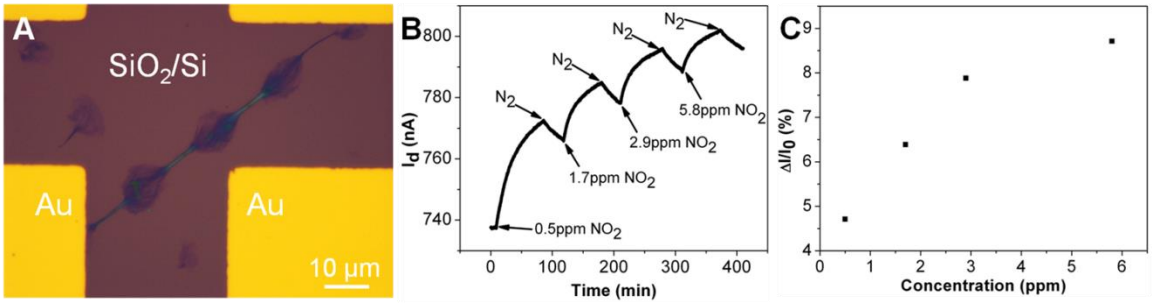

Figure 4 - 16. Gas sensing device made of a single beaded rGO string with gold electrodes. (A) Optical image of a single beaded rGO string device. (B) Real-time current response upon exposure of NO_2 at room temperature at various concentrations. (C) Graph of current change percentage *vs* NO_2 gas concentration.[102] Reprinted with permission from John Wiley and Sons.

4.2.5 Short Summary

In summary, this section has reported production of novel GO architecture on hydrophilic-hydrophobic SAMs micro-patterns on gold-coated SiO_2/Si by molecular combing of GO sheets. Various pattern sizes and shape of SAMs covered region can be easily created by micro-contact printing and therefore dictate the resulting sizes and shape of GO architectures. The fabricated beaded GO string, GO line and GO network have been fabricated and showed stability with feature size varied from 2 μm to 20 μm. NO_2 gas sensor based on a single beaded rGO string is also produced with 5.8 ppb detection limit.

4.3 Fabrication of Graphene Oxide (GO) Scroll Mesh

4.3.1 Introduction

In the previous section, production of GO scroll on hydrophobic substrate by molecular combing has been demonstrated.[18] After reduction, rGO scroll has shown good conductivity and its' potential to be used in electronics. In addition, recent report on graphene in mesh/network configuration as electrode has shown GO mesh with much higher transparency compared to its GO film counterpart.[93] Since, GO scrolls with high density and various length of up to 100 μm are able to be formed after molecular combing of GO sheets. Therefore, it is possible to form mesh/network configuration with GO scrolls as building block.

In this section, we report a fabrication of GO scroll mesh by combining molecular combing and transfer technique. As reported previously, high density of GO scrolls can be produced easily by molecular combing of high concentration GO sheets in aqueous solution. Molecular combing of GO sheets is performed separately in both horizontal and vertical

directions. By transferring the resulted GO scroll mesh on flexible substrate such as PET and reducing it into rGO scroll mesh; a flexible, conductive and highly transparent electrode can be produced. Stability of flexible rGO scroll mesh is also demonstrated through multiple bending tests.

4.3.2 Synthesis and Characterization of GO/rGO Scroll Mesh

Details of GO scroll mesh fabrication method are described in section 3.5.1. Briefly, high-density GO scrolls in vertical and horizontal directions are fabricated by molecular combing of GO sheets, separately. Vertical GO scrolls are then transferred onto horizontal GO scrolls to form mesh/network configuration as described in the section 3.5.1.[98] Schematic diagram of the fabrication of GO scroll mesh is shown in Figure 3 - 3. After transfer is completed, well connected vertically and horizontally aligned GO scrolls can be observed as shown in Figure 4 - 17A. High density GO scrolls are seen to be made of various width and length. These interconnecting GO scrolls are also observed over larger region and thus formed GO scroll mesh as shown in optical image in Figure 4 - 17B. In the other hand, in the case of direct molecular combing of GO sheets on horizontal direction followed by vertical direction combing on a single OTS-SiO_2/Si; it is observed that a second molecular combing in vertical direction yields a very low density of GO scroll (Figure 4 - 18). These GO scrolls did not formed a well-connected network and thus non-conductive. This observation is most expected due to decrease in hydrophobic surface area available since most has been covered by the existing horizontal GO scrolls during first combing. Reduced interaction between GO sheets and hydrophobic substrate decreased the

production of GO scrolls. Therefore, additional transfer step of vertical GO scrolls on horizontal GO scrolls is performed to result in well-connected GO scroll mesh.

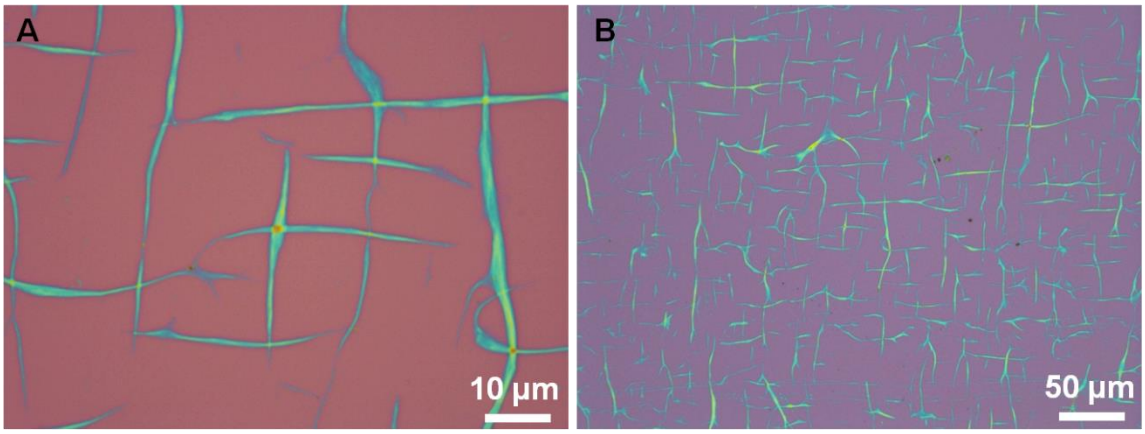

Figure 4 - 17. (A) High magnification and (B) Low magnification optical images of GO scroll mesh produced by combination of molecular combing of GO sheets and transfer of GO scrolls.

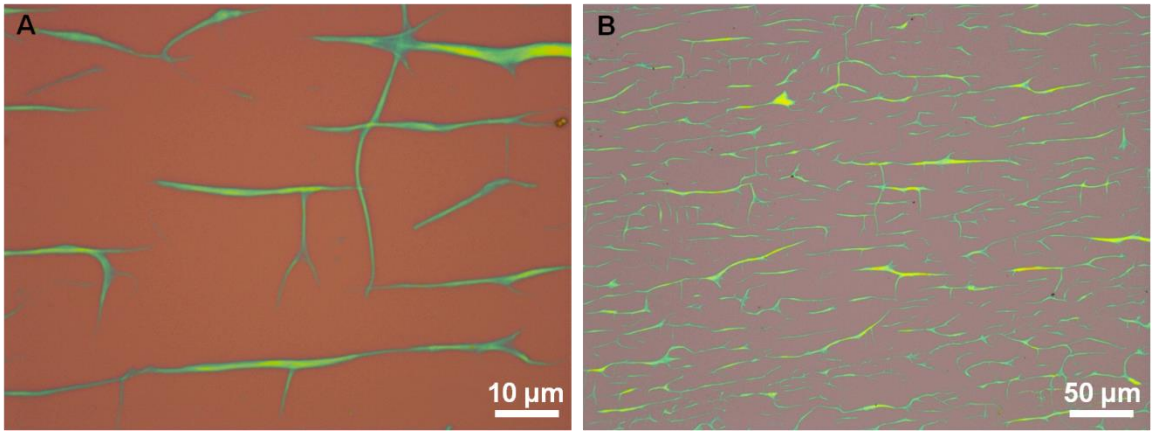

Figure 4 - 18. (A) High magnification and (B) Low magnification optical images of incomplete GO scroll mesh produced by molecular combing of GO sheets in horizontal direction and subsequently vertical direction on the same OTS-SiO_2/Si substrate.

The prepared GO scroll mesh on SiO_2/Si can then be characterized with Raman spectroscopy and AFM as depicted in Figure 4 - 19. Figure 4 - 19A shows optical image with interconnected GO scrolls which are chosen for Raman characterization. Raman mapping is performed in the preferred area which depicted high intensity of characteristics Raman bands of graphene oxide as shown in Figure 4 - 19B. Raman D band at 1353 cm^{-1} and Raman G band at 1606 cm^{-1} is observed for GO scroll (Figure 4 - 19C). Figure 4 - 19C also shown Raman spectra which are measured on a single GO scroll (marked by blue square on Figure 4 - 19B) and on junction of two GO scrolls (marked by red square on Figure 4 - 19B). No Raman peak shift is observed between single GO scroll and junction of two scrolls. In the other hand, both Raman D and G band intensity are higher at GO scroll junction compared to intensity at single GO scroll as seen from Figure 4 - 19C. This is highly due to the laser spot size of ~1 µm which also probed on the neighbor GO scroll at junction area which contribute to higher Raman peaks intensity. GO scroll morphology is observed by imaging with AFM which is shown in Figure 4 - 19D,E. AFM images supported the observation from optical microscopy, in which GO scroll mesh consists of GO scrolls in various widths and lengths are observed to be well connected to form mesh configuration. A section of GO scroll height is measured to be ~44 nm while GO scroll junction height is measured as ~84 nm as shown in inset of Figure 4 - 19E. In comparison to GWF[88] and graphene mesh[93] reported previously, GO scroll mesh prepared in this section is organized by stacking high density GO scrolls therefore larger GO coverage area and smaller spacing.

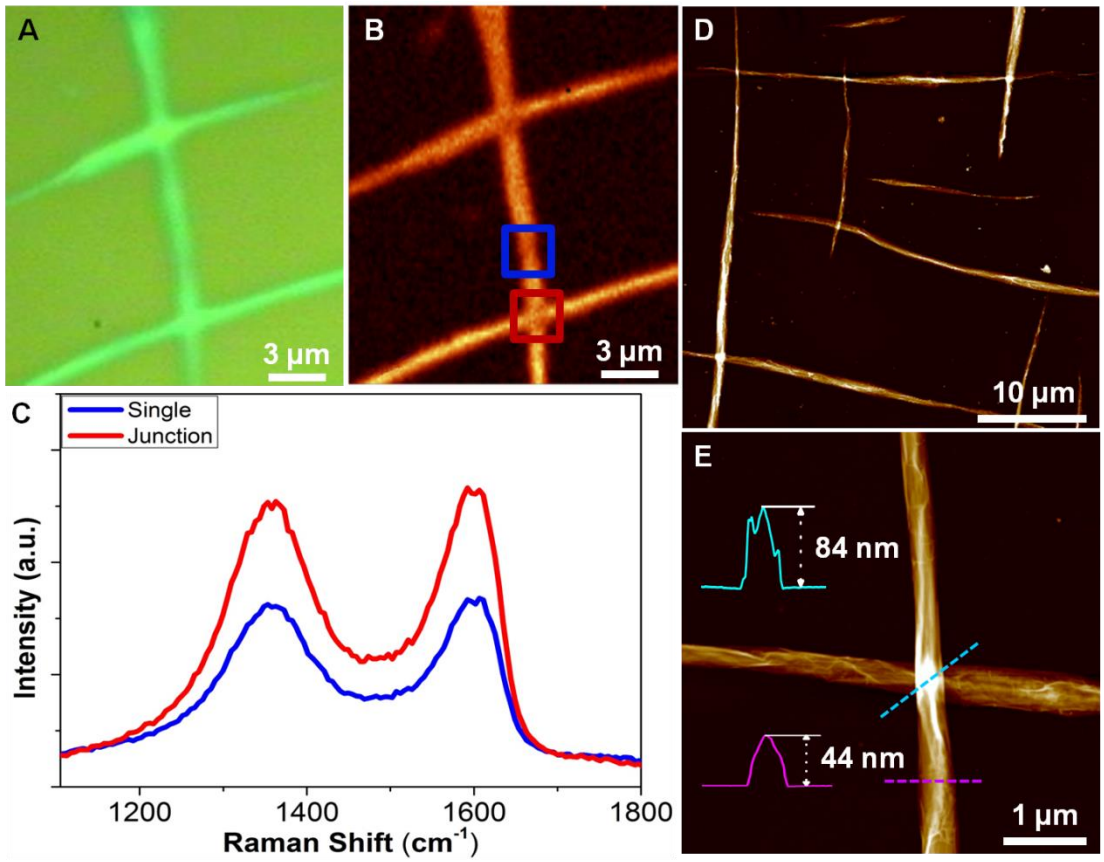

Figure 4 - 19. Raman and AFM characterizations of GO scroll mesh. (A) Optical and (B) Raman mapping images of interconnected GO scroll. (C) Raman signal of corresponding interconnected GO scroll shown in (B) on the junction (marked by red square) and on the single GO scroll (marked by blue square). (D) AFM image of GO scroll mesh (E) Higher magnification AFM image showing vertical GO scroll on top of horizontal GO scroll. Inset: height profile of a GO scroll (magenta line) and GO scroll junction (cyan line).

Graphene with its high conductivity and its high transparency has potential to be used in transparent electronics. Therefore, the transparency and conductivity of GO scroll mesh is investigated. In order to measure GO scroll mesh's optical transparency, GO scroll mesh need to be transferred on transparent substrate, glass slide. Figure 4 - 20A,B show

optical images of GO scroll mesh on glass slide substrate. GO scroll mesh is shown to be transferred successfully on glass slide over large area. Scrolling nature of GO is still maintained after transfer as seen from Figure 4 - 20A,B. Transferred GO scroll mesh on glass slide is subjected to reduction with hydrazine vapor at 70 ^{o}C overnight and thermal annealing at 200 ^{o}C for 5 h in H_2/Ar environment to increase GO scroll mesh conductivity.[135] Optical transparency of GO and rGO scroll mesh on glass slides are measured over wide wavelength range from 300 to 3300 nm as shown in Figure 4 - 20C. In the range of 500 to 3300 nm, GO scroll mesh before reduction demonstrates highest transmittance of more than 98% consistently over wide wavelength range. After reduction of GO scroll mesh with hydrazine vapor, its optical transmittance is measured to be ~95% which is slightly lower than GO scroll mesh. Additional reduction process by thermal annealing, improved the transmittance of rGO scroll mesh to ~97% (see inset Figure 4 - 20C). The transmittance improvement after additional reduction step is most likely due to the increase in graphitization.[136] Excellent transmittance of over 95% for both GO/rGO scroll mesh is attributed due to its mesh/network configuration which provide ample of vacant areas compared to its fully covered GO film.

After reduction, rGO scroll mesh's sheet resistance is measured with four-point probe. Sheet resistance measurement is carried out and averaged on more than 10 different points on rGO scroll mesh. Average sheet resistance of rGO scroll mesh which is reduced with hydrazine vapor and rGO scroll mesh which is reduced with combination of hydrazine vapor and thermal annealing are ~1.5 and 0.8 kΩ/sq, respectively. Additional reduction step of thermal annealing at 200 ^{o}C for 5 h has improved the conductivity of rGO scroll mesh. Compared to other rGO based flexible electrodes,[85-86, 93, 135, 137-139] the prepared GO/rGO

scroll mesh has shown superior transmittance and sheet resistance properties of 95% and ~1.5 kΩ/sq.

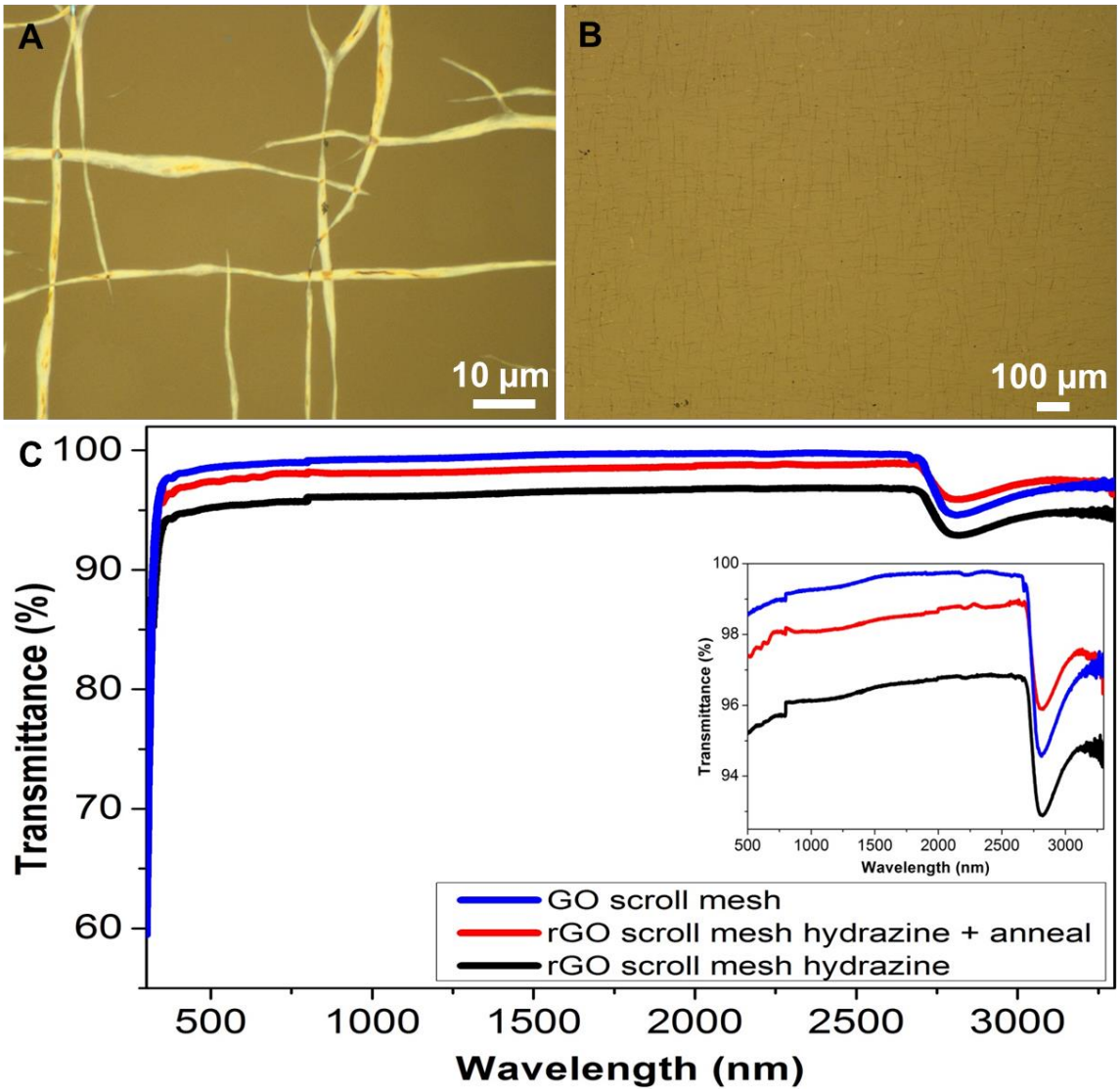

Figure 4 - 20. Transparency of GO/rGO scroll mesh. (A-B) Optical images of GO scroll mesh after transfer to transparent glass slides. (C) Transmittance of GO and rGO scroll mesh in the wavelength range of 300 - 3300 nm. Inset: Transmittance measurement in wavelength of 500 - 3300 nm.

4.3.3 rGO Scroll Mesh as Flexible Electrode

As described in the previous section above, the prepared rGO scroll mesh has outstanding optical transparency and low sheet resistance. rGO scroll mesh provides an alternative to be used in flexible electronics. GO scroll mesh is transferred to flexible substrate of polyethylene terephthalate (PET) with thickness of 0.1 mm and reduced with hydrazine vapor. Silver paste is affixed on rGO scroll mesh as electrodes as observed in Figure 4 - 21A. In flat condition, rGO scroll mesh device with channel width of ~1.8 cm exhibits good conductivity as shown in Figure 4 - 21B. In order to investigate the stability of rGO scroll mesh as flexible device, bending tests under different conditions are performed. rGO scroll mesh device resistance is measured at bend with bending radius of 20.5, 13.5 and 7.5 mm. As observed in Figure 4 - 21C, the device is stable with a little change in resistance of ~1.1% at bending radius 7.5 mm. The rGO scroll mesh based device is subjected to 10,000 bending cycles with bending radius of 13.5 mm. Figure 4 - 21D shows that there is no considerable alteration of resistance even after rGO scroll mesh is subjected to 8,000 bending cycles. As bending reached 10,000 cycles, the device resistance increase up to ~7%. Hence, rGO scroll mesh has shown exceptional stability during bending, thus makes it desirable to be used as flexible electrodes.

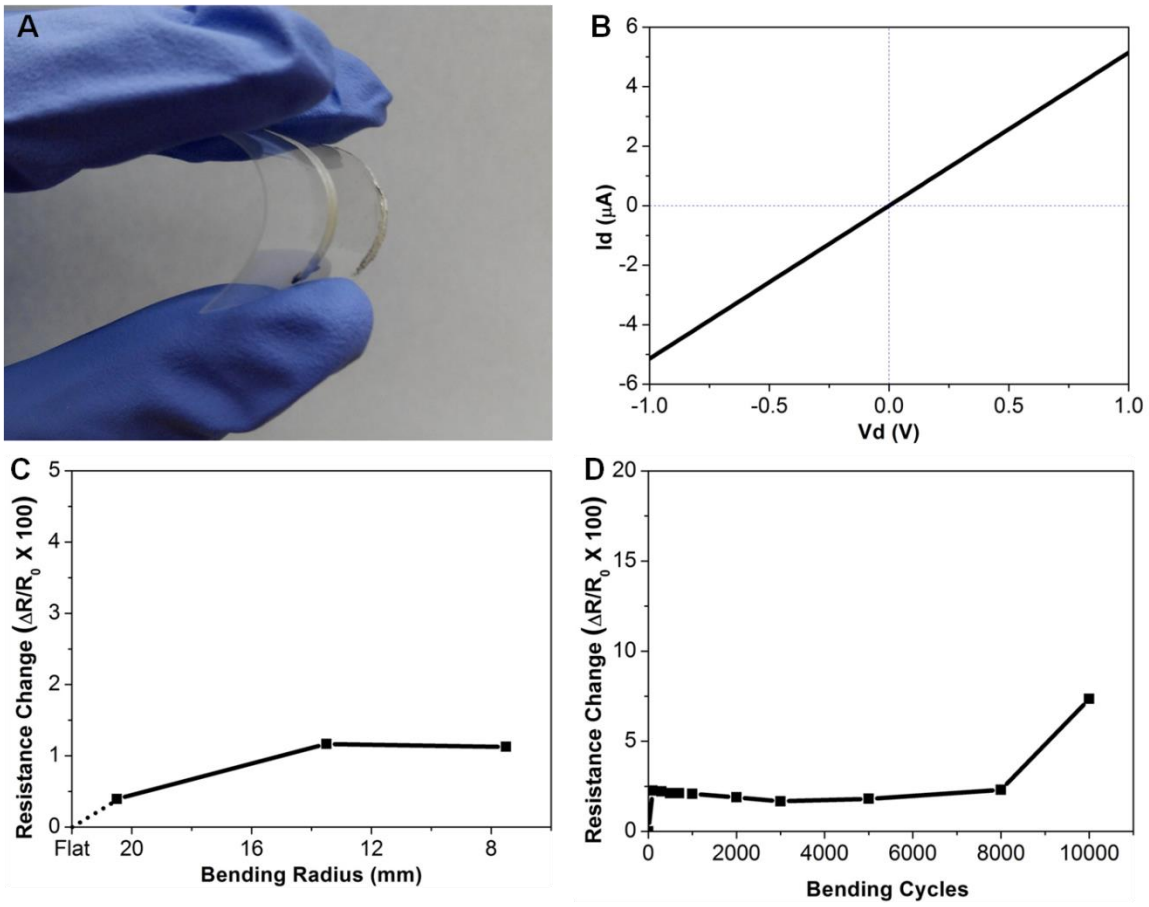

Figure 4 - 21. Electrical property characterization of rGO scroll mesh. (A) Optical image of rGO scroll mesh device on PET. (B) I_d-V_d of rGO scroll mesh device shown in (A). (C) Resistance change of rGO scroll mesh device at bending radius of 20.5, 13.5 and 7.5 mm. (D) Resistance change of rGO scroll mesh device after bending of up to 10,000 cycles at radius of 13.5 mm.

4.3.4 Short Summary

In summary, we described the first report on the production of GO/rGO scroll mesh via molecular combing combined with transfer technique. High density of GO scrolls enable the fabrication of well-connected GO scroll in mesh/network configuration. Its mesh

configuration contributed to its outstanding optical transparency in comparison to GO film. GO/rGO scroll mesh demonstrated outstanding properties with more than 95% transparency coupled with sheet resistance as low as ~0.8 kΩ/sq. The fabricated rGO scroll mesh has notably shown excellent electrical stability during bending at various bending radius and able to withstand 10,000 bending cycles. GO/rGO scroll mesh is successfully fabricated and demonstrated as feasible transparent and flexible electrodes.

Chapter 5:

Conclusions and Recommendations

5.1 Conclusions

In this thesis, molecular combing technique has been used in two-dimensional materials system to fabricate individual graphene oxide (GO) scroll. Other GO architectures, such as beaded GO string and GO in cross pattern, are achieved with molecular combing on hydrophilic-hydrophobic patterned substrates. High-density GO scrolls arranged in vertical and horizontal directions are stacked as building blocks for preparation of GO scroll mesh.

A first observation of molecular combing performed on two-dimensional material system is reported. Molecular combing of GO sheets in aqueous solution on hydrophobic substrates is performed to get GO scrolls. Individual GO scroll aligned in the direction of molecular combing process is easily produced as characterized by optical microscopy. Loosely scrolled and well aligned GO scrolls with various lengths are successfully fabricated on various hydrophobic substrates. Density of produced GO scrolls can be easily tuned by controlling the concentration of GO sheets in aqueous solution. The substrate's hydrophobicity and water as solvent of GO sheet solution are the key factors in the fabrication of GO scrolls. After reduction of GO scroll with hydrazine vapor, the obtained rGO scroll is able to detect NO_2 gas in real time with detection limit of 56 ppb. Overall, a simple and efficient technique has been developed to produce GO scroll via molecular combing.

Au substrate is easily patterned by micro-contact printing to form hydrophilic and hydrophobic self-assembled monolayer (SAM) patterns. Molecular combing performed with GO sheets in aqueous solution on the patterned substrate results in novel GO architectures. Beaded GO string is obtained on the MHA dot pattern surrounded by hydrophobic ODT region. By varying hydrophilic pattern feature, the obtained GO architecture can be easily controlled. In addition, it is observed that GO sheets have shown preference on hydrophilic region over hydrophobic region. Therefore, GO sheets reside on hydrophilic region when molecular combing is performed on hydrophilic-hydrophobic substrate with line and cross MHA pattern features. Importantly, GO sheets size, concentration of GO sheets and molecular combing speed effect on the formation of beaded GO strings are investigated. When the size of GO sheets size is smaller compared to the hydrophilic pattern, GO sheets are preferably confined within hydrophilic region. As concentration of GO sheets is increased and molecular combing speed is decreased, the density of formed GO scrolls formed is increased. Moreover, we demonstrate that the beaded GO string is still observed despite of hydrophilic functionality of SAMs. Gas sensor based on the reduced beaded GO string has shown the sensing capability on NO_2 gas. In comparison to the rGO scroll, reduced beaded GO string reveals enhanced detection limit of NO_2 (5.8 ppb).

Finally, the well connected GO scroll mesh is successfully fabricated for the first time through molecular combing of GO sheets combined with their stacking via our developed transfer method. High-density GO scrolls aligned in vertical and horizontal directions are fabricated separately by molecular combing in two directions, i.e. vertical and horizontal. The GO scroll mesh is obtained as vertical GO scrolls are transferred and

stacked on top of horizontal GO scrolls. Then it is transferred on transparent substrate, which shows excellent optical transparency and exceptional sheet resistance after it is reduced to rGO scroll mesh. The excellent transmittance of GO or rGO scroll mesh is attributed to its mesh/network structure. In addition, rGO scroll mesh on flexible substrate PET shows excellent electrical stability after multiple bending test. Therefore, the rGO scroll mesh can serve as practical transparent and flexible electrode.

5.2 Recommendations for Future Work

The present work reported molecular combing of GO sheets on hydrophobic substrate to fabricate GO scroll. Molecular combing of GO sheets is extended on hydrophilic-hydrophobic patterned substrate and results in novel GO architecture. High density and well aligned GO scroll and GO architectures can be easily fabricated with molecular combing. GO scroll mesh is fabricated by stacking high density GO scrolls aligned in vertical and horizontal direction. Further future works can be developed based on the work described in this thesis.

Firstly, in this thesis molecular combing has successfully fabricate GO scroll. However, the exact mechanism of GO scroll formation is not verified. Experimental method confirmed the importance of hydrophobic substrate and the solvent used to dissolve GO sheets. Simulation of the formation of GO scroll and or the scrolling process of GO sheets could provide a more accurate clarification of this process.

Secondly, molecular combing technique is successfully extended to two-dimensional material system of graphene. In addition, it is also possible to extend it to other two dimensional materials such as transition metal dichalcogenides (TMD) of MoS_2, WSe_2,

etc. Single layer MoS_2 is a semiconductor with direct band gap,[140] while single layer WSe_2 is a semiconductor with direct band gap but low intrinsic doping which exhibit ambipolar behaviour.[141] There are only limited reports on MoS_2 nanotube having metallic property[142] and MoS_2 nanotube with open end[143] have been shown. Similarly, other layered two-dimensional materials in scroll architecture might exhibit unique properties and hence fascinating to be studied. However, currently solution synthesis of other two-dimensional materials is limited with low yield and small sheets size. Small sheets size will limit the possibility of scroll formation via molecular combing. Other two-dimensional nanosheets and graphene oxide composite can be synthesized and scrolled by molecular combing. These composite scrolls can give rise to interesting and unexpected properties. In addition, incorporation of nanoparticles onto graphene oxide sheets during molecular combing will enable introduction of intercalants in GO scrolls. Size of intercalants will determine the intralayer distance in GO scrolls and open its possibility as hydrogen gas storage.

Thirdly, GO sheets is reported to show preference on hydrophilic area. Therefore, controlled placement of GO sheets on designated hydrophilic patterned area can be achieved. Stacked GO sheets with controlled pore size area can be fabricated by controlling the hydrophobic region size as described in section 4.2. This architecture is possible to be used as filtration membrane with selectivity over size.

Transparent and flexible GO scroll mesh is reported here to exhibit high electrical stability. However, future electronics development require stretchability in applications such as wearable electronics, wearable medical devices, etc. GO scroll mesh can be further transferred on stretchable substrates such as PDMS and GO scroll mesh based device

stability can be studied under uniaxial and biaxial stretch. Electrical conductivity of GO scroll mesh can also be enhanced via suitable reduction method.

REFERENCES

[1] K. S. Novoselov, A. K. Geim, S. V. Morozov, D. Jiang, Y. Zhang, S. V. Dubonos, I. V. Grigorieva, A. A. Firsov, *Science* **2004**, *306*, 666.

[2] A. A. Balandin, S. Ghosh, W. Bao, I. Calizo, D. Teweldebrhan, F. Miao, C. N. Lau, *Nano Lett.* **2008**, *8*, 902.

[3] C. Lee, X. Wei, J. W. Kysar, J. Hone, *Science* **2008**, *321*, 385.

[4] R. R. Nair, P. Blake, A. N. Grigorenko, K. S. Novoselov, T. J. Booth, T. Stauber, N. M. R. Peres, A. K. Geim, *Science* **2008**, *320*, 1308.

[5] C. G. Liu, Z. N. Yu, D. Neff, A. Zhamu, B. Z. Jang, *Nano Lett.* **2010**, *10*, 4863.

[6] J. J. Yoo, K. Balakrishnan, J. S. Huang, V. Meunier, B. G. Sumpter, A. Srivastava, M. Conway, A. L. M. Reddy, J. Yu, R. Vajtai, P. M. Ajayan, *Nano Lett.* **2011**, *11*, 1423.

[7] X. H. Cao, Y. M. Shi, W. H. Shi, G. Lu, X. Huang, Q. Y. Yan, Q. C. Zhang, H. Zhang, *Small* **2011**, *7*, 3163.

[8] S. Yang, X. Feng, S. Ivanovici, K. Müllen, *Angew. Chem. Int. Ed.* **2010**, *49*, 8408.

[9] G. X. Wang, X. P. Shen, J. Yao, J. Park, *Carbon* **2009**, *47*, 2049.

[10] D. Y. Pan, S. Wang, B. Zhao, M. H. Wu, H. J. Zhang, Y. Wang, Z. Jiao, *Chem. Mater.* **2009**, *21*, 3136.

[11] S. Patchkovskii, J. S. Tse, S. N. Yurchenko, L. Zhechkov, T. Heine, G. Seifert, *Proc. Natl. Acad. Sci. U.S.A.* **2005**, *102*, 10439.

[12] G. K. Dimitrakakis, E. Tylianakis, G. E. Froudakis, *Nano Lett.* **2008**, *8*, 3166.

[13] F. Schedin, A. K. Geim, S. V. Morozov, E. W. Hill, P. Blake, M. I. Katsnelson, K. S. Novoselov, *Nat. Mater.* **2007**, *6*, 652.

[14] J. T. Robinson, F. K. Perkins, E. S. Snow, Z. Wei, P. E. Sheehan, *Nano Lett.* **2008**, *8*, 3137.

[15] J. D. Fowler, M. J. Allen, V. C. Tung, Y. Yang, R. B. Kaner, B. H. Weiller, *ACS Nano* **2009**, *3*, 301.

[16] Q. Y. He, H. G. Sudibya, Z. Y. Yin, S. X. Wu, H. Li, F. Boey, W. Huang, P. Chen, H. Zhang, *ACS Nano* **2010**, *4*, 3201.

[17] X. H. Cao, Z. Y. Zeng, W. H. Shi, P. R. Yep, Q. Y. Yan, H. Zhang, *Small* **2013**, *9*, 1703.

[18] H. Li, J. Wu, X. Qi, Q. He, C. Liusman, G. Lu, X. Zhou, H. Zhang, *Small* **2013**, *9*, 382.

[19] J. Huang, J. Harvey, W. H. D. Fam, M. A. Nimmo, I. Y. A. Tok, *Procedia Eng.* **2013**, *60*, 195.

[20] X. Li, W. Cai, J. An, S. Kim, J. Nah, D. Yang, R. Piner, A. Velamakanni, I. Jung, E. Tutuc, S. K. Banerjee, L. Colombo, R. S. Ruoff, *Science* **2009**, *324*, 1312.

[21] D. Li, M. B. Muller, S. Gilje, R. B. Kaner, G. G. Wallace, *Nat. Nanotechnol.* **2008**, *3*, 101.

[22] W. S. Hummers, R. E. Offeman, *J. Am. Chem. Soc*. **1958**, *80*, 1339.

[23] S. Eigler, M. Enzelberger-Heim, S. Grimm, P. Hofmann, W. Kroener, A. Geworski, C. Dotzer, M. Röckert, J. Xiao, C. Papp, O. Lytken, H.-P. Steinrück, P. Müller, A. Hirsch, *Adv. Mater.* **2013**, *25*, 3583.

[24] A. K. Geim, K. S. Novoselov, *Nat. Mater.* **2007**, *6*, 183.

[25] T. Rabenau, A. Simon, R. K. Kremer, E. Sohmen, *Eur. Phys. J. B Condensed Matter* **1993**, *90*, 69.

[26] R. W. Lof, M. A. van Veenendaal, B. Koopmans, H. T. Jonkman, G. A. Sawatzky, *Phys. Rev. Lett.* **1992**, *68*, 3924.

[27] S. J. Tans, M. H. Devoret, H. Dai, A. Thess, R. E. Smalley, L. J. Geerligs, C. Dekker, *Nature* **1997**, *386*, 474.

[28] J. W. G. Wilder, L. C. Venema, A. G. Rinzler, R. E. Smalley, C. Dekker, *Nature* **1998**, *391*, 59.

[29] B. Partoens, F. M. Peeters, *Phys. Rev. B* **2006**, *74*, 075404.

[30] C. Virojanadara, M. Syväjarvi, R. Yakimova, L. I. Johansson, A. A. Zakharov, T. Balasubramanian, *Phys. Rev. B* **2008**, *78*, 245403.

[31] Y.-M. Lin, C. Dimitrakopoulos, K. A. Jenkins, D. B. Farmer, H.-Y. Chiu, A. Grill, P. Avouris, *Science* **2010**, *327*, 662.

[32] Y. Hernandez, V. Nicolosi, M. Lotya, F. M. Blighe, Z. Sun, S. De, I. T. McGovern, B. Holland, M. Byrne, Y. K. Gun'Ko, J. J. Boland, P. Niraj, G. Duesberg, S. Krishnamurthy, R. Goodhue, J. Hutchison, V. Scardaci, A. C. Ferrari, J. N. Coleman, *Nat. Nanotechnol.* **2008**, *3*, 563.

[33] M. Lotya, Y. Hernandez, P. J. King, R. J. Smith, V. Nicolosi, L. S. Karlsson, F. M. Blighe, S. De, Z. Wang, I. T. McGovern, G. S. Duesberg, J. N. Coleman, *J. Am. Chem. Soc.* **2009**, *131*, 3611.

[34] C. Vallés, C. Drummond, H. Saadaoui, C. A. Furtado, M. He, O. Roubeau, L. Ortolani, M. Monthioux, A. Pénicaud, *J. Am. Chem. Soc.* **2008**, *130*, 15802.

[35] X. Li, G. Zhang, X. Bai, X. Sun, X. Wang, E. Wang, H. Dai, *Nat. Nanotechnol.* **2008**, *3*, 538.

[36] N. Liu, F. Luo, H. Wu, Y. Liu, C. Zhang, J. Chen, *Adv. Funct. Mater.* **2008**, *18*, 1518.

[37] K. S. Kim, Y. Zhao, H. Jang, S. Y. Lee, J. M. Kim, K. S. Kim, J.-H. Ahn, P. Kim, J.-Y. Choi, B. H. Hong, *Nature* **2009**, *457*, 706.

[38] P. W. Sutter, J.-I. Flege, E. A. Sutter, *Nat. Mater.* **2008**, *7*, 406.

[39] W. Gao, L. B. Alemany, L. Ci, P. M. Ajayan, *Nat. Chem.* **2009**, *1*, 403.

[40] I. K. Moon, J. Lee, R. S. Ruoff, H. Lee, *Nat. Commun.* **2010**, *1*, 73.

[41] V. Dua, S. P. Surwade, S. Ammu, S. R. Agnihotra, S. Jain, K. E. Roberts, S. Park, R. S. Ruoff, S. K. Manohar, *Angew. Chem. Int. Ed.* **2010**, *49*, 2154.

[42] M. Zhou, Y. Wang, Y. Zhai, J. Zhai, W. Ren, F. Wang, S. Dong, *Chem. Eur. J.* **2009**, *15*, 6116.

[43] H.-L. Guo, X.-F. Wang, Q.-Y. Qian, F.-B. Wang, X.-H. Xia, *ACS Nano* **2009**, *3*, 2653.

[44] M. J. McAllister, J.-L. Li, D. H. Adamson, H. C. Schniepp, A. A. Abdala, J. Liu, M. Herrera-Alonso, D. L. Milius, R. Car, R. K. Prud'homme, I. A. Aksay, *Chem. Mater.* **2007**, *19*, 4396.

[45] G. Williams, B. Seger, P. V. Kamat, *ACS Nano* **2008**, *2*, 1487.

[46] L. J. Cote, R. Cruz-Silva, J. Huang, *J. Am. Chem. Soc.* **2009**, *131*, 11027.

[47] X. Xie, L. Ju, X. Feng, Y. Sun, R. Zhou, K. Liu, S. Fan, Q. Li, K. Jiang, *Nano Lett.* **2009**, *9*, 2565.

[48] L. M. Viculis, J. J. Mack, R. B. Kaner, *Science* **2003**, *299*, 1361.

[49] S. F. Braga, V. R. Coluci, S. B. Legoas, R. Giro, D. S. Galvão, R. H. Baughman, *Nano Lett.* **2004**, *4*, 881.

[50] G. Mpourmpakis, E. Tylianakis, G. E. Froudakis, *Nano Lett.* **2007**, *7*, 1893.

[51] Y. Chen, J. Lu, Z. Gao, *J. Phys. Chem. C* **2007**, *111*, 1625.

[52] V. R. Coluci, S. F. Braga, R. H. Baughman, D. S. Galvão, *Phys. Rev. B* **2007**, *75*, 125404.

[53] F. Zeng, Y. Kuang, G. Liu, R. Liu, Z. Huang, C. Fu, H. Zhou, *Nanoscale* **2012**, *4*, 3997.

[54] Y. Gao, X. Chen, H. Xu, Y. Zou, R. Gu, M. Xu, A. K. Y. Jen, H. Chen, *Carbon* **2010**, *48*, 4475.

[55] J. Zheng, H. Liu, B. Wu, Y. Guo, T. Wu, G. Yu, Y. Liu, D. Zhu, *Adv. Mater.* **2011**, *23*, 2460.

[56] M. V. Savoskin, V. N. Mochalin, A. P. Yaroshenko, N. I. Lazareva, T. E. Konstantinova, I. V. Barsukov, I. G. Prokofiev, *Carbon* **2007**, *45*, 2797.

[57] F. Zeng, Y. Kuang, Y. Wang, Z. Huang, C. Fu, H. Zhou, *Adv. Mater.* **2011**, *23*, 4929.

[58] Y.-K. Kim, D.-H. Min, *Carbon* **2010**, *48*, 4283.

[59] G. Cheng, I. Calizo, X. Liang, B. A. Sperling, A. C. Johnston-Peck, W. Li, J. E. Maslar, C. A. Richter, A. R. Hight Walker, *Carbon* **2014**, *76*, 257.

[60] A. Bensimon, A. Simon, A. Chiffaudel, V. Croquette, F. Heslot, D. Bensimon, *Science* **1994**, *265*, 2096.

[61] H. Yokota, F. Johnson, H. B. Lu, R. M. Robinson, A. M. Belu, M. D. Garrison, B. D. Ratner, B. J. Trask, D. L. Miller, *Nucleic Acids Res.* **1997**, *25*, 1064.

[62] X. Michalet, R. Ekong, F. Fougerousse, S. Rousseaux, C. Schurra, N. Hornigold, M. v. Slegtenhorst, J. Wolfe, S. Povey, J. S. Beckmann, A. Bensimon, *Science* **1997**, *277*, 1518.

[63] J. F. Allemand, D. Bensimon, L. Jullien, A. Bensimon, V. Croquette, *Biophys. J.* **1997**, *73*, 2064.

[64] J. Li, C. Bai, C. Wang, C. Zhu, Z. Lin, Q. Li, E. Cao, *Nucleic Acids Res.* **1998**, *26*, 4785.

[65] Z. X. Deng, C. D. Mao, *Nano Lett.* **2003**, *3*, 1545.

[66] M. Oshige, K. Yamaguchi, S.-i. Matsuura, H. Kurita, A. Mizuno, S. Katsura, *Anal. Biochem.* **2010**, *400*, 145.

[67] T. Heim, T. Melin, D. Deresmes, D. Vuillaume, *Appl. Phys. Lett.* **2004**, *85*, 2637.

[68] G. Liu, J. Zhao, *Langmuir* **2006**, *22*, 2923.

[69] H. Nakao, H. Hayashi, T. Yoshino, S. Sugiyama, K. Otobe, T. Ohtani, *Nano Lett.* **2002**, *2*, 475.

[70] A. Nayak, A. K. Dutta, G. Belfort, *Biochem. Biophys. Res. Commun.* **2008**, *369*, 303.

[71] B. Moores, E. Drolle, S. J. Attwood, J. Simons, Z. Leonenko, *PLoS ONE* **2011**, *6*, e25954.

[72] S. Li, X. Huang, H. Li, H. Cai, C. L. Gan, F. Boey, H. Zhang, *Small* **2010**, *6*, 2708.

[73] D. Tian, Y. Song, L. Jiang, *Chem. Soc. Rev.* **2013**, *42*, 5184.

[74] S. D. Gillmor, A. J. Thiel, T. C. Strother, L. M. Smith, M. G. Lagally, *Langmuir* **2000**, *16*, 7223.

[75] A. N. Efremov, E. Stanganello, A. Welle, S. Scholpp, P. A. Levkin, *Biomaterials* **2013**, *34*, 1757.

[76] Z. Huang, P. C. Wang, J. Feng, A. G. MacDiarmid, Y. Xia, G. M. Whitesides, *Synth. Met.* **1997**, *85*, 1375.

[77] R. K. Smith, P. A. Lewis, P. S. Weiss, *Prog. Surf. Sci.* **2004**, *75*, 1.

[78] G. Lu, W. Li, J. Yao, G. Zhang, B. Yang, J. Shen, *Adv. Mater.* **2002**, *14*, 1049.

[79] S. Palacin, P. C. Hidber, J.-P. Bourgoin, C. Miramond, C. Fermon, G. M. Whitesides, *Chem. Mater.* **1996**, *8*, 1316.

[80] Z. Zhong, B. Gates, Y. Xia, D. Qin, *Langmuir* **2000**, *16*, 10369.

[81] Y. Wang, D. Maspoch, S. Zou, G. C. Schatz, R. E. Smalley, C. A. Mirkin, *Proc. Natl. Acad. Sci. U.S.A.* **2006**, *103*, 2026.

[82] C. Bechinger, H. Muffler, C. Schäfle, O. Sundberg, P. Leiderer, *Thin Solid Films* **2000**, *366*, 135.

[83] A. Kumar, G. M. Whitesides, *Appl. Phys. Lett.* **1993**, *63*, 2002.

[84] L. W. James, K. Amit, A. B. Hans, K. Enoch, M. W. George, *Nanotechnol.* **1996**, *7*, 452.

[85] Z. Yin, S. Sun, T. Salim, S. Wu, X. Huang, Q. He, Y. M. Lam, H. Zhang, *ACS Nano* **2010**, *4*, 5263.

[86] E. Kymakis, K. Savva, M. M. Stylianakis, C. Fotakis, E. Stratakis, *Adv. Funct. Mater.* **2013**, *23*, 2742.

[87] L. Gomez De Arco, Y. Zhang, C. W. Schlenker, K. Ryu, M. E. Thompson, C. Zhou, *ACS Nano* **2010**, *4*, 2865.

[88] X. Li, P. Sun, L. Fan, M. Zhu, K. Wang, M. Zhong, J. Wei, D. Wu, Y. Cheng, H. Zhu, *Sci. Rep.* **2012**, *2*, 395.

[89] X. Li, R. Zhang, W. Yu, K. Wang, J. Wei, D. Wu, A. Cao, Z. Li, Y. Cheng, Q. Zheng, R. S. Ruoff, H. Zhu, *Sci. Rep.* **2012**, *2*, 870.

[90] Y. Wang, L. Wang, T. Yang, X. Li, X. Zang, M. Zhu, K. Wang, D. Wu, H. Zhu, *Adv. Funct. Mater.* **2014**, *24*, 4666.

[91] X. Lee, T. Yang, X. Li, R. Zhang, M. Zhu, H. Zhang, D. Xie, J. Wei, M. Zhong, K. Wang, D. Wu, Z. Li, H. Zhu, *Appl. Phys. Lett.* **2013**, *102*, 163117.

[92] X. Zang, Q. Chen, P. Li, Y. He, X. Li, M. Zhu, X. Li, K. Wang, M. Zhong, D. Wu, H. Zhu, *Small* **2014**, *10*, 2583.

[93] Q. Zhang, X. Wan, F. Xing, L. Huang, G. Long, N. Yi, W. Ni, Z. Liu, J. Tian, Y. Chen, *Nano Res.* **2013**, *6*, 478.

[94] M. A. Meitl, Z. T. Zhu, V. Kumar, K. J. Lee, X. Feng, Y. Y. Huang, I. Adesida, R. G. Nuzzo, J. A. Rogers, *Nat. Mater.* **2006**, *5*, 33.

[95] X. S. Li, Y. W. Zhu, W. W. Cai, M. Borysiak, B. Y. Han, D. Chen, R. D. Piner, L. Colombo, R. S. Ruoff, *Nano Lett.* **2009**, *9*, 4359.

[96] A. Reina, H. Son, L. Jiao, B. Fan, M. S. Dresselhaus, Z. Liu, J. Kong, *J. Phys. Chem. C* **2008**, *112*, 17741.

[97] L. Y. Jiao, B. Fan, X. J. Xian, Z. Y. Wu, J. Zhang, Z. F. Liu, *J. Am. Chem. Soc.* **2008**, *130*, 12612.

[98] H. Li, J. Wu, X. Huang, Z. Yin, J. Liu, H. Zhang, *ACS Nano* **2014**, *8*, 6563.

[99] X. Zhou, X. Huang, X. Qi, S. Wu, C. Xue, F. Y. C. Boey, Q. Yan, P. Chen, H. Zhang, *J. Phys. Chem. C* **2009**, *113*, 10842.

[100] H. Li, J. Zhang, X. Zhou, G. Lu, Z. Yin, G. Li, T. Wu, F. Boey, S. S. Venkatraman, H. Zhang, *Langmuir* **2009**, 26, 5603.

[101] H. Li, Y. Xia, J. Wu, Q. He, X. Zhou, G. Lu, L. Shang, F. Boey, S. S. Venkatraman, H. Zhang, *ACS Appl. Mater. Interfaces* **2012**, *4*, 687.

[102] J. Wu, H. Li, X. Qi, Q. He, B. Xu, H. Zhang, *Small* **2014**, *10*, 2239.

[103] L. V. Radushkevich, V. M. Lukyanovich, *Zurn. Fisic. Chim.* **1952**, *26*, 88.

[104] S. Iijima, *Nature* **1991**, *354*, 56.

[105] D. S. Bethune, C. H. Klang, M. S. de Vries, G. Gorman, R. Savoy, J. Vazquez, R. Beyers, *Nature* **1993**, *363*, 605.

[106] A. L. Kalamkarov, A. V. Georgiades, S. K. Rokkam, V. P. Veedu, M. N. Ghasemi-Nejhad, *Int. J. Solids Struct.* **2006**, *43*, 6832.

[107] W. Zhou, J. Liu, T. Chen, K. S. Tan, X. Jia, Z. Luo, C. Cong, H. Yang, C. M. Li, T. Yu, *Phys. Chem. Chem. Phys.* **2011**, *13*, 14462.

[108] X. Shi, Y. Cheng, N. M. Pugno, H. Gao, *Small* **2010**, *6*, 739.

[109] X. Shi, N. M. Pugno, Y. Cheng, H. Gao, *Appl. Phys. Lett.* **2009**, *95*, 163113.

[110] X. Shi, Y. Cheng, N. M. Pugno, H. Gao, *Appl.Phys. Lett.* **2010**, *96*, 053115.

[111] U. Mirsaidov, V. R. S. S. Mokkapati, D. Bhattacharya, H. Andersen, M. Bosman, B. Ozyilmaz, P. Matsudaira, *Lab Chip* **2013**, *13*, 2874.

[112] H. Kudo, K. Suga, M. Fujihira, *Chem. Lett.* **2007**, *36*, 298.

[113] K. W. Bewig, W. A. Zisman, *J. Phys. Chem.* **1965**, *69*, 4238.

[114] T. Smith, *J. Colloid Interf. Sci.* **1980**, *75*, 51.

[115] F. Tuinstra, J. L. Koenig, *J. Chem. Phys.* **1970**, *53*, 1126.

[116] K. N. Kudin, B. Ozbas, H. C. Schniepp, R. K. Prud'homme, I. A. Aksay, R. Car, *Nano Lett.* **2007**, *8*, 36.

[117] E. P. Bellido, J. M. Seminario, *J. Phys. Chem. C* **2010**, *114*, 22472.

[118] C. Py, P. Reverdy, L. Doppler, J. Bico, B. Roman, C. N. Baroud, *Phys. Rev. Lett.* **2007**, *98*, 156103.

[119] X. Guo, H. Li, B. Yeop Ahn, E. B. Duoss, K. J. Hsia, J. A. Lewis, R. G. Nuzzo, *Proc. Natl. Acad. Sci. U.S.A.* **2009**, *106*, 20149.

[120] B. Annegret, M. Michael, P. Wolfgang, *Nanotechnol.* **2011**, *22*, 035304.

[121] J. Guan, L. J. Lee, Proceedings of the National Academy of Sciences of the United States of America **2005**, *102*, 18321.

[122] O. Leenaerts, B. Partoens, F. M. Peeters, *Phys. Rev. B* **2008**, *77*, 125416.

[123] J. Zhang, A. Boyd, A. Tselev, M. Paranjape, P. Barbara, *Appl. Phys. Lett.* **2006**, *88*, 123112.

[124] L. Ganhua, E. O. Leonidas, C. Junhong, *Nanotechnol.* **2009**, *20*, 445502.

[125] H. Y. Jeong, D.-S. Lee, H. K. Choi, D. H. Lee, J.-E. Kim, J. Y. Lee, W. J. Lee, S. O. Kim, S.-Y. Choi, *Appl. Phys. Lett.* **2010**, *96*, 213105.

[126] J. L. Wilbur, A. Kumar, E. Kim, G. M. Whitesides, *Adv. Mater.* **1994**, *6*, 600.

[127] Y. Xia, M. Mrksich, E. Kim, G. M. Whitesides, *J. Am. Chem. Soc.* **1995**, *117*, 9576.

[128] H.-J. Butt, K. Graf, M. Kappl, *Physics and Chemistry of Interfaces*, Wiley-VCH Verlag GmbH & Co. KGaA, **2004**.

[129] J. Rafiee, X. Mi, H. Gullapalli, A. V. Thomas, F. Yavari, Y. Shi, P. M. Ajayan, N. A. Koratkar, *Nat. Mater.* **2012**, *11*, 217.

[130] U. S. E. P. Agency, Vol. *75*, *Government Printing Office*, **2010**, 6473.

[131] Z. Jijun, B. Alper, H. Jie, L. Jian Ping, *Nanotechnol.* **2002**, *13*, 195.

[132] H. Chang, J. D. Lee, S. M. Lee, Y. H. Lee, *Appl. Phys. Lett.* **2001**, *79*, 3863.

[133] J. Li, Y. Lu, Q. Ye, M. Cinke, J. Han, M. Meyyappan, *Nano Lett.* **2003**, *3*, 929.

[134] L. Valentini, I. Armentano, J. M. Kenny, C. Cantalini, L. Lozzi, S. Santucci, *Appl. Phys. Lett.* **2003**, *82*, 961.

[135] G. Eda, G. Fanchini, M. Chhowalla, *Nat. Nanotechnol.* **2008**, *3*, 270.

[136] X. Wang, L. Zhi, K. Müllen, *Nano Lett.* **2007**, *8*, 323.

[137] Q. He, S. Wu, S. Gao, X. Cao, Z. Yin, H. Li, P. Chen, H. Zhang, *ACS Nano* **2011**, *5*, 5038.

[138] S. Pei, J. Zhao, J. Du, W. Ren, H.-M. Cheng, *Carbon* **2010**, *48*, 4466.

[139] S.-K. Lee, H. Y. Jang, S. Jang, E. Choi, B. H. Hong, J. Lee, S. Park, J.-H. Ahn, *Nano Lett.* **2012**, *12*, 3472.

[140] K. F. Mak, C. Lee, J. Hone, J. Shan, T. F. Heinz, *Phys. Rev. Lett.* **2010**, *105*, 136805.

[141] J.-K. Huang, J. Pu, C.-L. Hsu, M.-H. Chiu, Z.-Y. Juang, Y.-H. Chang, W.-H. Chang, Y. Iwasa, T. Takenobu, L.-J. Li, *ACS Nano* **2013**, *8*, 923.

[142] M. Remskar, A. Mrzel, M. Virsek, M. Godec, M. Krause, A. Kolitsch, A. Singh, A. Seabaugh, *Nanoscale Res. Lett.* **2011**, *6*, 26.

[143] F. Hoshyargar, A. Yella, M. Panthöfer, W. Tremel, *Chem. Mater.* **2011**, *23*, 4716.

LIST OF PUBLICATIONS

Journals

- **J. Wu**, H. Li, X. Y. Qi, Q. Y. He, B. Xu and H. Zhang, Graphene Oxide Architectures Prepared by Molecular Combing on Hydrophilic-Hydrophobic Micropatterns, Small 10 (11), 2239 **(2014)**
- **J. Wu**, H. Li, Z. Y. Yin, J. Q. Liu, X. H. Cao and H. Zhang, Layer Thinning and Etching of Mechanically Exfoliated MoS_2 Nanosheets by Thermal Annealing in Air, Small 9 (19), 3314 **(2013)**
- H. Li, **J.Wu**, X. Huang, Z. Y. Yin, J. Q. Liu, H. Zhang, A Universal, Rapid Method for Clean Transfer of Nanostructures onto Various Substrates, ACS Nano, 8 (7), 6563 **(2014)** (**Equal contribution to 1st author**)
- H. Li, **J. Wu**, X. Huang, G. Lu, J. Yang, X. Lu, Q. H. Xiong and H. Zhang, Rapid and Reliable Thickness Identification of Two-dimensional Nanosheets using Optical Microscopy, ACS Nano 7 (11), 10344 **(2013)** (**Equal contribution to 1st author**)
- H. Li, **J. Wu**, X. Y. Qi, Q. Y. He, C. Liusman, G. Lu, X. Z. Zhou and H. Zhang, Graphene Oxide Scrolls on Hydrophobic Substrates Fabricated by Molecular Combing and Their Application in Gas Sensing, Small 9 (3), 382 **(2013)** (**Equal contribution to 1st author**)
- Z. Y. Yin, X. Zhang, Y. Q. Cai, J. Z. Chen, J. I. Wong, Y. Y. Tay, J. W. Chai, **J. Wu**, Z. Y. Zeng, B. Zheng, H. Y. Yang and H. Zhang, Preparation of MoS_2-MoO_3

Hybrid Nanomaterials for Light-Emitting Diodes, Angewandte Chemie International Edition, DOI: 10.1002/anie.201402935 **(2014)**

- H. Li, **J. Wu**, Z. Y. Yin and H. Zhang, Preparation and Applications of Mechanically Exfoliated Single- and Multi-layer MoS_2 and WSe_2 Nanosheets, Accounts of Chemical Research 47, 1067 **(2014)**
- H. Li, X. Y. Qi, **J. Wu**, Z. Y. Zeng, J. Wei and H. Zhang, Investigation of MoS_2 and Graphene Nanosheets by Magnetic Force Microscopy, ACS Nano 7 (3), 2842 **(2013)**
- Y. Y. Zhao, X. Luo, H. Li, J. Zhang, P. T. Araujo, C. K. Gan, **J. Wu**, H. Zhang, S. Y. Quek, M. S. Dresselhaus and Q. H. Xiong, Interlayer breathing and shear modes in few-trilayer MoS_2 and WSe_2, Nano Letters 13, 1007 **(2013)**
- H. Li, Y. Xia, **J. Wu**, Q. Y. He, X. Z. Zhou, G. Lu, L. Shang, F. Boey, S. S. Venkatraman and H. Zhang, Surface Modification of Smooth Poly(l-lactic acid) Films for Gelatin Immobilization, ACS Applied Materials & Interfaces 4 (2), 687 **(2012)**
- C. Liusman, H. Li, G. Lu, **J. Wu**, F. Boey, S. Z. Li and H. Zhang, Surface-Enhanced Raman Scattering of Ag-Au Nanodisk Heterodimers, The Journal of Physical Chemistry C 116 (18), 10390 **(2012)**.

Conference Presentations

- European Materials Research Society (E-MRS) 2014 Spring Meeting, *Oral Presentation*, Lille-France May 2014. Winner of Young Scientist Award 2014 Symposium G "Carbon- or Nitrogen-containing Nanostructured Thin Films"
- New Diamond and Nano Carbons Conference, *Poster Presentation*, Singapore May 2013.
- Small Sciences Symposium, Frontiers in Nanomedicine, *Poster Presentation*, Singapore Dec. 2012.
- UK-Singapore Materials Workshop, Materials for Tomorrow, *Poster Presentation*, Singapore Dec. 2012.